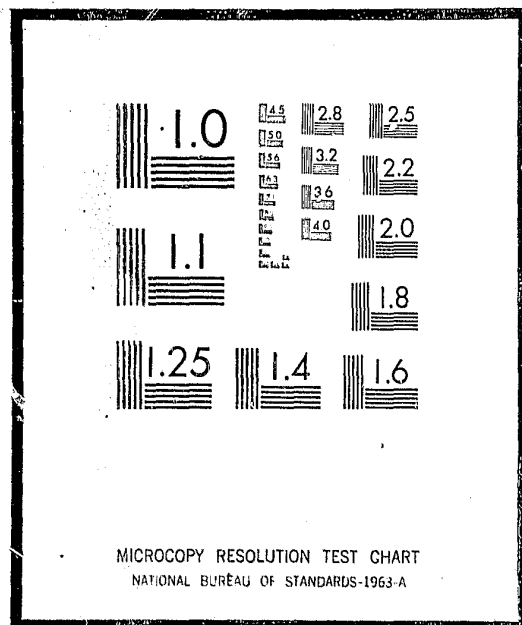


NCJRS

This microfiche was produced from documents received for inclusion in the NCJRS data base. Since NCJRS cannot exercise control over the physical condition of the documents submitted, the individual frame quality will vary. The resolution chart on this frame may be used to evaluate the document quality.



Microfilming procedures used to create this fiche comply with the standards set forth in 41CFR 101-11.504

Points of view or opinions stated in this document are those of the author(s) and do not represent the official position or policies of the U.S. Department of Justice.

U.S. DEPARTMENT OF JUSTICE
LAW ENFORCEMENT ASSISTANCE ADMINISTRATION
NATIONAL CRIMINAL JUSTICE REFERENCE SERVICE
WASHINGTON, D.C. 20531

6/7/76

Date filmed

FINAL REPORT

AN INVESTIGATION OF THE FEASIBILITY OF USE OF LASER OPTOACOUSTIC DETECTION FOR THE DETECTION OF EXPLOSIVES

Prepared by

Case Western Reserve University
Cleveland, Ohio 44106

April 1975

Prepared for

The Aerospace Corporation
El Segundo, California

Aerospace Subcontract No. 44343-V

This project was supported by Contract Number J-LEAA-025-73 awarded by the National Institute of Law Enforcement and Criminal Justice, Law Enforcement Assistance Administration, U.S. Department of Justice, under the Omnibus Crime Control and Safe Streets Act of 1968, as amended. Points of view or opinions stated in this document are those of the authors and do not necessarily represent the official position or policies of the U.S. Department of Justice.

LIST OF CONTENTS

	Page
1. Introduction	1
2. Summary of Results	3
3. Feasibility Investigations	5
Basic Component Investigation	5
Investigation of Interfering Species	12
Determination of Optoacoustic Spectra of Explosives Vapor In the Presence of Interfering Species	13
4. Feasibility Determinations	14
5. Recommendations	21

1. Introduction

This document is the final technical report on work carried out for the United States Department of Justice, National Institute of Law Enforcement and Criminal Justice, Law Enforcement Assistance Administration, Washington, D.C. (LEAA).

This program was part of a larger program managed by The Law Enforcement Group of the Aerospace Corporation, El Segundo, California, for LEAA under Contract No. J-LEAA-025-73. This actual program constituted a subcontract (No. 44343-V) with The Aerospace Corporation.

The objective of this investigation was to determine the feasibility of using a laser optoacoustic device to detect the presence of minute quantities of trace vapors emitted by various explosives.

The motivation for this study is the need for a method of detecting the presence of explosives without extensive search and without disturbance of the explosives. An effective remote detection method would be a great deterrent to both illegal and unauthorized use of explosives.

The overall function of such a detection and monitoring method might correspond in many respects to that of metal detection methods used at airports to deter the carrying of concealed weapons made of metal. The outlines of characteristically shaped weapons carried in baggage can be revealed through the use of X-ray machines. This method is effective only in the case of dense materials such as metals. At the present time, the detection of explosives is much more difficult since the substances are not particularly dense nor necessarily of any one specific shape.

Commercial explosives and detonators might be made more easily detectable by various means of "tagging." If the tagging method consists in fact

of impregnation of some component by a specific gas, such as SF_6 , for example, the explosive and/or the detonator might be detected optoacoustically through detection of the "taggant".

The optoacoustic method is not new. It has been known for years that it is possible to focus radiation onto a body of gas, to heat it up slightly and to generate a pressure wave in the gas. The pressure wave can be detected with a sensitive microphone and this type of system is used in industry either to monitor the presence of the gas or the level of the incident radiation. This method is particularly sensitive if the incident radiation is strongly absorbed by the gas.

Despite this long and commonplace history, this method took on new dimensions with the advent of tunable lasers and in the new configuration, the method is not only sensitive but specific since each molecular species has its own optoacoustic "signature" as the laser is tuned over ten or more appropriate wavelengths.

The results of this investigation indicate that the optoacoustic method can be used effectively for the detection of explosives. A summary of the principal results is presented in Section 2 of this report.

In as much as it is meaningful, this report follows the task designation and language of the original proposal submitted by Case Western Reserve University. All departures from the original plan were either clearly dictated by the nature of the intermediate results or were agreed to by both Aerospace Corporation and Case Western Reserve University so as to ensure attainment of the principal objectives of this investigation.

Details of equipment, experimental methods and results are presented in Section 3. The significance of these results is discussed in Section 4 and recommendations for further action are presented in Section 5.

2. Summary of Results

(Note: this is not a summary of all the work performed but rather a summary of principal significant results.)

1. In the absence of interfering species, nitroglycerine (NG) ethylene glycol dinitrate (EGDN) and dinitrotoluene (DNT) can be unmistakably detected in the 6 micron, 9 micron and 11 micron wavelength regions.
2. Interfering species can be divided into two categories: one being environmental and the other being associated with the sample. Atmospheric "pollutants" such as NO , NO_2 , CH_4 , water vapor, iso-butane and normal butane are examples of the first category and shoe polish, shaving lotion, and water entrained in hygroscopic samples are examples of the latter.

In so far as environmental interfering species are concerned, NG, EGDN, and DNT can be detected best in the 9μ wavelength region, using a mixed isotope CO_2 laser. It is estimated that trinitrotoluene can be detected in that region also. In the 6μ wavelength region (CO laser), both NO_2 and water vapor cause troublesome interference. In the 9.8μ to 11μ wavelength region, butane vapors are troublesome. For all such cases, the effect of these troublesome interferences can be alleviated if necessary by use of differential, double path, detection methods. However, these wavelength regions should perhaps be avoided in favor of the $9.2\mu \sim 9.7\mu$ and the $11\mu \sim 12\mu$ wavelength regions where normally, there is no interference from environmental interfering species. Radiation at these wavelength regions are available from mixed isotope CO_2 lasers such as those used in the present investigation.

3. The presence of SF_6 vapor emitted by a simulated blasting cap and by pieces of Teflon impregnated over a year ago with SF_6 , were readily detected with an optoacoustic detector using radiation in the 10.6μ wavelength region. The signals were so strong that neither environmental nor sample related interfering species would cause significant degradation. More specifically, the peak values of the optoacoustic signals were $714 \mu V/mW$ and $4 \mu V/mW$ for the blasting cap and the Teflon capsules respectively. The strongest interfering signal was of the order of $\leq 0.5 \mu V/mW$, resulting in a signal to noise ratio of at least 8.
4. Optoacoustic detection is as sensitive for explosives as for small molecules such as SF_6 , except perhaps for ring structures small as DNT and TNT. It is likely that much vibrational energy gets trapped in other intramolecular vibrational modes and is not available for heating up the gas through vibrational-translational energy transfer. In this context, for the larger molecules, it is meaningless to talk of rejection ratios. More constructively, wavelength regions need to be chosen so as to avoid interfering species. That is possible with the use of mixed isotope CO_2 lasers which are now available in sealed-off long lived configuration.

On the other hand, SF_6 is so strongly efficient that it does have a very high rejection ratio.

5. The results of this present investigation indicate that a portable, field operable, long lived, laser optoacoustic detector can be implemented. Preliminary estimates indicate that power consumption in the operating mode is likely to be less than 200 watts, overall weight is

likely to be less than 100 lbs (separable into 2 or 3 component parts of less than 40 lbs each, with dimensions comparable to those of small suitcases or backpacks used by hikers.)

6. The principal recommendation is that a one year amendment program be implemented without delay to further define the parameters for optimum detection modes in the $9.2\mu \sim 9.8\mu$ and the $11\mu \sim 12\mu$ wavelength regions for explosives and in the 10.6μ wavelength region for SF_6 , and to yield a prototype unit with characteristics in overall agreement with those delineated above in item 5.

3. Feasibility Investigation

3.1 Basic Component Investigation

3.1.1 Optoacoustic Detection Method: Underlying Principles and Experimental Techniques

In the context of the present investigation, the presence of minute quantities of explosives vapor in a "carrier" gas such as air or nitrogen, is detected by exposing the gas mixture to monochromatic infrared radiation. This incident radiation is absorbed by the explosives molecule which store the energy internally in the form of vibrational energy. Non-resonant collisions with carrier gas molecules result in transfer of the internal vibrational energy (in the explosives molecule) to the molecules of the carrier gas, in the form of external translational energy. This becomes manifest in the form of minute increases in temperature and pressure. If the incident radiation is modulated, sound waves are produced in the gas and these can be detected with very sensitive microphones.

The two basic molecular processes just described and two other competing processes are illustrated schematically in Figure 1. Absorption is illustrated as Process 1 and vibrational-translational (V-T) energy transfer is shown as Process 3. In the present context, the magnitude of the optoacoustic signal can be significantly decreased by the competing effects of Processes (2) and (4). In process (2), intermolecular collision results in spontaneous emission, i.e., fluorescence rather than V-T energy transfer, whereas in process (4), vibrational energy is trapped internally and degraded from one vibrational mode into another until all phase relationship with the modulation reference signal is lost.

In the interest of completeness, a simple rate equation description of the optoacoustic process is provided in Appendix 1. Equation (9) of that account yields the result that the magnitude of the optoacoustic signal is proportional to

$$\frac{1}{2} \frac{\tau_C^{-2} B N I_0}{(B I_0 + \tau^{-1})^2} \quad \text{where}$$

N = number explosive vapor molecules/cm³

I_0 = intensity of incident radiation in watt/cm²/sec

B = Einstein Coefficient For Stimulated Absorption and Emission

$$\tau^{-1} = \tau_C^{-1} + \tau_R^{-1}$$

τ_C^{-1} = rate of de-excitation due to collisions

τ_R^{-1} = rate of de-excitation due fluorescence

This result indicates that optimum conditions are attained when $BI_0 = \tau^{-1}$. Since, in practice, near standard conditions, τ_R^{-1} is not likely to be larger

than 10^5 whereas τ_C^{-1} is not likely to be less than 10^6 , this means that for optimum conditions $BI_0 \approx \tau_C^{-1}$ meaning that it is not useful to excite molecules at a rate higher than we can de-excite by V-T transfer. In fact, if BI_0 exceeds τ^{-1} greatly, the signal actually starts to decrease as $\frac{1}{I_0}$! These considerations are illustrated schematically in Figure 2. Indicated also is the fact that for a variety of reasons, there is also an initial dead zone and no optoacoustic signal is detected for power levels below threshold.

A block diagram of the apparatus used in this investigation is exhibited in Figure 3.

Two types of lasers, the CO and CO₂ lasers, were used in determining the optoacoustic spectra of the explosives. The CO laser used in this investigation was a sealed-off dry ice cooled, grating tuned device using ¹²C¹⁶O as the lasing gas. The laser could be tuned from well below 5.8 microns to above 6.6 microns, with output power ranging from a few hundred milliwatts at the shorter wavelengths to about 70 milliwatts at 6.6 microns. It was initially felt that to achieve single line operation at wavelengths greater than 6μ, it would be necessary to use ¹³C¹⁸O as the lasing gas. After considerable effort, it was discovered that whereas ¹²C¹⁸O could be operated satisfactorily in the sealed-off mode, the isotope ¹³C¹⁸O as supplied, contained impurities in significant quantities and sealed-off operation could not be sustained. The cost of the ¹³C¹⁸O isotope prohibits flowing operation. Fortunately at about that time, operating techniques had been sufficiently developed so that significant single line power could be obtained with ¹²C¹⁸O up to 6.626 microns. Further increases in wavelength being of no interest, it was agreed* that efforts to use ¹³C¹⁸O would be discontinued. While operation with this

* CWRU and Aerospace.

gas proved to be unsatisfactory because of impurities in the rare isotope gas, this approach proved unnecessary when the required wavelengths were obtained using the $^{12}\text{C}^{16}\text{O}$ isotope. The fifteen wavelengths used in this part of the study spanned the region from 5.837 microns and 6.626 microns and are listed in Table 1.

Excitation in the 9 micron and 11 micron regions was obtained using two CO_2 lasers. In the 9 micron region, a flowing gas, water cooled, grating tuned laser using $^{12}\text{C}^{16}\text{O}_2$ as the active medium was used. Eight wavelengths ranging from 9.25 microns to 9.71 microns, with powers to 1 watt, were used in this region. These are also listed in Table 1.

In the 11 micron region a sealed-off, water cooled, grating tuned laser containing a mixture of $^{12}\text{C}^{16}\text{O}_2$ and $^{13}\text{C}^{16}\text{O}_2$ was used for excitation. The seven wavelengths, spanning the region from 10.75 microns to 11.19 microns, which were used in this part of the investigation are listed in Table 1.

The optoacoustic detector used for this work is a high sensitivity device of a proprietary design. Sodium chloride windows are used to permit entrance and exit of the exciting radiation. The cell is capable of being evacuated to a moderate vacuum (~ 1 Torr) to enable rapid and positive removal of vapors between sample runs. Heater coils are provided to permit operation at elevated temperatures. The detectivity of the cell was measured using SF_6 excited with 10.571 micron radiation. The cell was shown to detect 1 part in 10^6 SF_6 in air with a signal to noise ratio of 10^5 , indicating an extrapolated sensitivity of at least 1 part in 10^9 (vapor phase) or approximately 1 part in 10^{12} at liquid density.

The exciting radiation was chopped with a variable rate mechanical chopper and all signal measurements were done using standard phase sensi-

tive techniques with reference to the chopping frequency. Signal amplification and detection was accomplished with a Keithley Instruments Model 427 Current Amplifier and a PAR Model HR-8 Lock-In Amplifier. Laser power measurements were made with a Coherent Radiation Model 210 Power Meter.

All explosives spectra were taken with a small sample placed inside the cell. In most instances, the cell was evacuated with the explosive sample in place, after which the cell was filled with dry nitrogen or with air or with air containing some interfering species. In all measurements, since a closed system was used, it was assumed that the explosive vapors were at thermal equilibrium with the source.

Initially, use of brass optoacoustic cells and long stretches of copper tubing was accompanied by the absence of any optoacoustic signal. This was interpreted, correctly, as being due to excessive adsorption of the explosives molecules on the cell walls. Subsequent investigations were carried out with the cells heated to about 45°C . Further investigations with cell and explosives at room temperature ($\approx 23^\circ\text{C}$) indicated that these explosives can also be detected at room temperature, the ratios of signals at the two temperatures being in fact very nearly equal to the ratio of the vapor pressures at the two temperatures.

3.1.2 Reproducibility and Linearity of Signals

A measure of the quality of the data obtained in this investigation was obtained by detecting NG in air using eleven different CO_2 lines in the 10.6μ wavelength region, all at 50 mw power level. Each of the readings was repeated four times after all parameters had been adjusted arbitrarily to

other readings and then reset to the original values. The results obtained from that exercise are tabulated in Table II. It is seen that the root mean square value of the deviation from perfect reproducibility is 4.8%. The average is closer to 3%, there being two large errors 9.6% and 5.9% which are responsible for the root mean square deviation being larger. It is estimated that with electronically controlled plasma current modulation rather than mechanical modulation, with appropriate narrow band filtering at the pre-amp stage and with feedback control on the laser power supply, this type of error can be reduced to less than 1.5%.

Linearity of the signal with respect to the incident radiation power level is of interest, since interpretation of data is simplified if it can be shown that increase in population density would merely result in a proportional increase in the magnitude of the optoacoustic signal. Similarly, spectra of interfering species can then be added to the spectra of explosives vapors in a linear manner. To investigate this possibility, optoacoustic signals for NG and air were obtained at twenty different CO_2 transition wavelengths in the $10 \sim 11\mu$ wavelength region for incident power levels ranging from 20 mw to 350 mw. The normalized signals are plotted versus power level in Figure 4. At low power levels, "dead zone" behavior could be detected; in the 60 mw to 300 mw range, the normalized response curves were reasonably flat indicating linear response. There seemed to be indication of saturation for some of the highly absorbed lines. The overall behavior indicates, however, that linear superposition of signals would not result in grossly misleading conclusions. The data are presented in Figure 4.

3.1.3 Initial Considerations of Vapor Pressure and Absorption Spectra

Standard moderate resolution infrared absorption spectra were collected

for the four explosives NG, EGDN, DNT and TNT as well as for some additional commercial preparations such as PETN, TOVEX and ROX. These spectra as well as corresponding spectra for NO , NO_2 , CH_4 , isobutane and normal butane are exhibited in Appendix 2. A summary of these absorptions of interest in the present context is provided schematically in Figure 4. The wavelength regions at which discrete laser outputs can be obtained are also indicated in this figure.

Measured and/or extrapolated values for the vapor pressures of the four explosives of principal interest were obtained from the literature^{1,2}. These values are shown in Figure 4. These values indicate that at room temperature, equilibrium number densities are $1.25 \times 10^{14}/\text{cc}$, $5.28 \times 10^{14}/\text{cc}$ and $1.25 \times 10^{12}/\text{cc}$ for EGDN, DNT and NG respectively.

3.1.4 Optoacoustic Spectra of Explosives

Optoacoustic spectra were obtained by placing the explosive sample in the cell, evacuating it to less than one torr pressure and then filling the cell with dry nitrogen. The letter of the original contract specified that spectra of the explosives alone were also to be investigated. Initially this was done for three explosives but no signals were obtained. Previous experience with other gases had indicated that whereas high resolution spectra could be obtained with gases at pressure less than 1 Torr, the optoacoustic signal was usually three or four orders of magnitude smaller than when a "carrier" gas was used with the sample. In addition, in the context of the intended application, the optoacoustic signal of interest would be that generated with the explosive vapor in air. In view of these considerations, it was agreed* that all optoacoustic spectra would be obtained with dry nitrogen.

* CWRU and Aerospace

The 6 μ Wavelength Region

In practice, the commercially supplied dry nitrogen yielded a background optoacoustic signal in the 6 μ wavelength region, not characteristic of water vapor but similar to that of NO₂. This background was subtracted from the explosive vapor optoacoustic spectra in all cases.

Optoacoustic spectra for the 6 μ wavelength region for the vapors of NG, EGDN and DNT are exhibited in Figures 6, 7 and 8. The average laser power, measured at the input of the cell was 10 mw at each wavelength. Spectra of TN, RDX, PETN and TOVEX are shown in Figures 9, 10, 11 and 12 respectively. (It may be mentioned at this point that comparison of these spectra with that for water vapor suggests that in all these four cases, the observed spectra are primarily due to water vapor. For RDX, PETN and TOVEX, the water vapor signal is too large to be due to water vapor in the laboratory air. Water must have been present entrained in the explosives samples.) Spectrum for a low NG content dynamite is shown in Figure 13. Data exhibited in these figures are also available in numerical form in Table III.

Optoacoustic spectra for the 9 μ wavelength region for vapors of NG, EGDN, DNT, Dynamite and black powder are shown in Figures 14, 15, 16, 17 and 18 respectively. The corresponding data are presented in Table IV.

In the 11 μ wavelength region, optoacoustic spectra were obtained for vapors of NG and EGDN for 45°C and for 23°C. The spectra are shown plotted in Figures 19, 20 and 22 respectively and the corresponding data are presented in numerical form in Table V.

3.2 Investigation of Interfering Species

It was agreed that the interfering species to be investigated would be

butane, methane, NO₂, NO and water vapor. These were investigated in both the 6 μ and 9 μ wavelength regions.

For the 6 μ wavelength region, the concentrations for the samples used are listed in Table VI and optoacoustic spectra data are listed in Table VII. The spectra are shown plotted in Figures 14 - 18.

In the 9 μ wavelength region, none of the listed interfering species yielded any optoacoustic signal except for butane. The optoacoustic spectrum for butane is shown in Figure 23.

3.3 Determination of Optoacoustic Spectra of Explosives Vapor In The Presence of Interfering Species

Our extensive exploration of additional transitions in the 9 μ and 11 μ wavelength region did not leave us with sufficient time to perform all the tasks of the contract to the letter. However, all the required spectra of the listed interfering species had indeed been obtained and the results of our investigation of the validity of superposition of spectra allow us to draw conclusions from the two separate families of spectra. Furthermore, and this was really the most compelling reason, data listed in Tables 5 and 6, clearly show that interference due to water vapor renders the 6 μ wavelength region marginal at best for optoacoustic detection of explosives vapors. Although interference from NO₂ alone might threaten to render detection of DNT ineffective, the added effect of the omnipresent water vapor is much, much worse. Therefore for the 6 μ wavelength region, optoacoustic spectra of vapors of EGDN, NG and DNT in the presence of water vapor have been synthesized from actual (but separately determined) optoacoustic spectra. Figure 19 illustrates that it is relatively easy to detect EGDN at room

temperature at 50% RH. As shown in Figures 20 and 21, the situation is less happy for NG and circumstances are definitely not favorable for DNT. Relative humidity of 50% would be unacceptable for the last case.

4. Feasibility Determination

In this section we report on the results of an evaluation of whether it is indeed feasible to use optoacoustics to detect the presence of explosives. We base our evaluation on data reported in previous sections, on additional data to be reported in this section and on experience obtained during a field operation of a portable optoacoustic unit.

Some of the basic considerations included in our evaluation are those of

- a. Intrinsic optoacoustic efficiency
- b. Basic difficulties due to interference
- c. Ultimate limitations imposed by technology
- d. Cost, reliability and ease of operation.

We have listed in Table VIII, a quantity which serves as a figure of merit in so far as optoacoustic detection is concerned. It is the maximum normalized optoacoustic signal detected (that is, microvolts of signal per milliwatt of incident radiation) for a vapor with a concentration of 1 part per million. The actual figures listed in Table VIII are valid only for the specific CO transitions used in this investigation.

Optoacoustic Efficiency

Referring to Table VIII, we see that the optoacoustic efficiencies of the explosives EGDN and NG are comparable to those of smaller molecules but that

of DNT is lower. It is not possible to conclude on the basis of this data alone whether ring structures do enhance internal vibrational energy trapping, resulting in lower optoacoustic efficiency, or whether the lower value for DNT is due to smaller absorption coefficients. However, the values listed in Table VIII indicate that there is nothing drastically wrong with the optoacoustic response of the explosives EGDN, NG and DNT. We are not certain about TNT. Since most of the six micron wavelength region work was carried out with only about 10 milliwatt of incident power, there is much opportunity for enhancement of the signal. Similar conclusions are equally valid for the data obtained in the nine and eleven micron wavelength regions.

Interference

As mentioned in previous sections, interference may arise because of other molecular systems present in the environment or because of substances which are entrained with the explosives. In the 6 micron wavelength region, NO, NO₂ and water vapor give rise to interference of varying degrees of difficulty depending on the explosives involved. However it is water vapor which is most troublesome. It is interesting to note that for the 6 μ transitions used in this investigation, water is in fact very inefficient optoacoustically speaking, the signal being 0.001 $\mu\text{v}/\text{mw}/\text{ppm}$ as compared with 8.55 $\mu\text{v}/\text{mw}/\text{ppm}$ for NG, 1.114 $\mu\text{v}/\text{mw}/\text{ppm}$ for EGDN and 0.05 $\mu\text{v}/\text{mw}/\text{ppm}$ for DNT respectively. However, there are many water molecules in air even at "low" relative humidity and the resulting interference is not negligible. (See Figure 32, for example).

We note however that if the water vapor is present in the environment, the optoacoustic signal from that background can be determined separately and subtracted from the combined signal. In practice this would be carried out using two optoacoustic cells. A single incident beam is split and the

two portions are directed with the two detector cells. The resulting water vapor background signals are adjusted so that no coherent AC optoacoustic signal is obtained in the absence of the explosive. The explosive optoacoustic signal alone is obtained as the laser tuned across (say) six different transitions. This same technique can be used to alleviate the interference effects due to other environmental interfering species. Using this common mode rejection scheme, it is anticipated that all the three explosives NG, EGDN and DNT can be detected for conditions equivalent to the vapor being in equilibrium with the explosive.

Of much greater concern are instances where the water seems to be entrained in the explosive and the vapor pressure of the explosive itself is low so that the water vapor optoacoustic signal dominates the output. This seems to be the situation for the explosives RDX, PETN and TOVEX. In the laboratory, there was some thought of removing the water from the explosives so that the optoacoustic signals of the explosives alone could be obtained. However inasmuch as some of these explosives are normally prepared in the form of water slurries, and furthermore inasmuch as in contemplated use at airports etc., there would not be opportunity for desiccating all luggage presented for inspection, this elaborate approach was abandoned for more practical ways of circumventing the interference problem. This was the principal reason for the additional work carried out at 9 and 11 microns. Investigations at those higher wavelengths show that there is no interference due to NO, NO₂, CH₄ or water vapor. However higher molecular weight hydrocarbons may be troublesome and butane constitutes an example. Again, dual cell, common mode rejection techniques may be used to circumvent the effects of environmental interfering species in the 9 - 12 micron wavelength region.

The principal components of an optoacoustic detector system are a laser, a radiation chopper, the detector cell itself and associated power supplies and signal processing electronics. Of all these ingredients, the only item which is questionable is the availability of a long lived sealed-off, extended tuning range CO laser. More specifically, the operating life expectancy should be above 5000 hrs. in sealed-off dry-ice cooled mode; power should be at least 1 watt when operated with a diffraction grating or its equivalent. Gain should be sufficiently high so that the tuning range extends to at least 6.6 microns. Although such a laser might be available at one or more laboratories, there is no accumulated experience regarding long-lived sealed-off CO lasers. In contrast to this, there is now sufficient collective experience to indicate without the question of a doubt that long-lived, sealed-off CO₂ lasers with mixed isotopes and extended tuning range can readily be implemented. This is a very good reason for serious thought to the 9 μ - 12 μ wavelength regions.

The detector cell is inherently a simple device and there is ample information in open literature regarding the principles guiding the design of such cells. Every laboratory will of course, develop its own preferred practice in cell design resulting in real or imagined improved performance. The results of our study suggest that the inner surfaces of the cell be heated to reduce adsorption but the temperature should not be so high as to degrade microphone performance. It is important to check the electronic saturation characteristics of such microphones.

Most of the data in the course of this investigation were taken using a mechanical light chopper. Mechanical choppers are adequate for the purpose but are often not very stable in the chopping frequency, do not provide simple harmonic modulation and often cannot provide modulation at sufficiently high

frequencies. At Case Western Reserve University, we find that more satisfactory modulation can be obtained via direct modulation of the laser plasma discharge current. Higher modulation frequencies and smaller cells can be obtained in this manner. Feedback control can also be used to ensure sinusoidal modulation. Reverting to the topic of cell design, it is worth mentioning at this point, that some cells have high acoustic Q but are not very sensitive to minor frequency deviations away from the resonant frequency. Other cells of more classic design have the disadvantage of having such sharp resonance curves that elaborate frequency stabilization is required if noise is to be kept to acceptable levels.

Cost, Reliability and Ease of Maintenance

Laser excited optoacoustic detector systems contemplated in this study are inherently simple systems. A rough estimate indicates that such systems may be produced for sale at a unit price of less than \$25,000 each. This price would vary somewhat depending on what additional signal processing and/or display features are required. Again CO systems might be troublesome because of the possible need for occasional refill. There is no such difficulty with sealed-off long-lived CO₂ lasers and it would seem that the CO₂ units can be operated with non-technical personnel.

More specifically, a typical CO₂ laser optoacoustic detector system would comprise of the following components with the indicated estimated power requirements, size and weight.

- a. The laser and cell assembly; including the coolant reservoir, thermoelectric cooler, beam splitter, common mode rejection dual cell assembly, diffraction grating for wavelength tuning, and

- piezoelectric transmission mirror for power optimization. Power requirement is approximately 200 watts, weight is estimated to be less than 50 lbs. and dimensions are of the order of 22" x 8" x 8".
- b. The power supply unit includes the high voltage power supply, discharge current modulation control, diffraction grating stepping motor supply and control and cavity dimension optimization supply and control. Dimensions are estimated to be of the order of 18" x 8" x 8". Weight is less than 50 lbs.
 - c. The data processing and display unit includes a current (pre) amplifier and a phase sensitive amplifier with a limited frequency tuning option. Logic for controlling the tuning sequence of the laser and means for processing the "signature" of the received signal are provided. A simple yes/no type of display (perhaps audio as well as visual) would probably be the principal output device. In addition a simple "profile" or "signature" readout device might also be desirable.

As this phase of the investigation neared the end as dictated by allotted time and funds, it became manifestly clear that the investigation had succeeded in revealing the nature of the possible problems and had also succeeded in establishing the directions in which some further limited additional investigations are indicated. To do the most good in the remaining time it was agreed* that we would not hold ourselves strictly to all the exact letter of the contract but proceed as rapidly as possible to reveal the possibilities

* CWRU and Aerospace.

available to us in the $9\mu \sim 11\mu$ wavelength region. For awhile this implied that we would not have the opportunity to carry out the test in public places such as an airport or a bus station. We were fortunate that we were able to secure the use of a more or less portable self contained CO_2 laser excited optoacoustic unit, constructed by CWRU for a local instrument company, and we were able to operate this unit for four days in a local instrument exhibit at the Convention Center in downtown Cleveland. The environment in that hall was less than optimum from a health standpoint but was excellent for our purposes. We were not allowed to bring explosives into that hall but were able to detect SF_6 at 10.6μ amidst all the gasoline fumes and other types of pollution. A view of the apparatus used in the laboratory investigations is provided in Figure 33a and a view of the field operable unit is provided in Figure 33b.

This field demonstration was of special significance in view of some additional work carried out at the suggestion of Aerospace. Three types of samples were tested to see if SF_6 emitted by these samples could be detected optoacoustic. As indicated by the results exhibited in Figure 34, the result was positive in all three cases. The first sample consisted of a metal simulated blasting cap. The SF_6 optoacoustic signal obtained in that case was overwhelmingly large, being $714 \mu\text{v}/\text{mw}$. The other two samples consisted of Teflon capsules impregnated with SF_6 sometime ago and estimated to be emitting SF_6 at extremely low rates perhaps at the rate of 1 - 5 nanoliters per minute. As shown in Figure 34, positive identification were obtained in both cases but the profile showed signs of saturation and the intensity of the incident radiation was probably too high for the purposes.

5. Recommendations

It is recommended that this initial promising investigation be followed up with an amendment so that the following activities and results might be pursued and attained.

- a. Optoacoustic spectra of explosives and of SF_6 be examined carefully in the $9\mu \sim 12\mu$ wavelength region using mixed isotope CO_2 lasers. The interference due to hydrocarbons (butane and higher molecular weight) such as those found in jet fuels need to be examined.
- b. The dual cell common-mode rejection technique be developed and used in all future investigations so as to yield more meaningful estimates of irreducible effects of interfering species.
- c. The 6μ wavelength region be re-examined with increased CO power and with the dual cell common-mode rejection technique.
- d. Detection be carried out with gas flowing through the detector cell.
- e. A field operable system be designed incorporating scanning and power optimization, narrow band filtering and phase sensitive amplification, and appropriate signal processing and display.
- f. A prototype of this field operable unit be implemented.

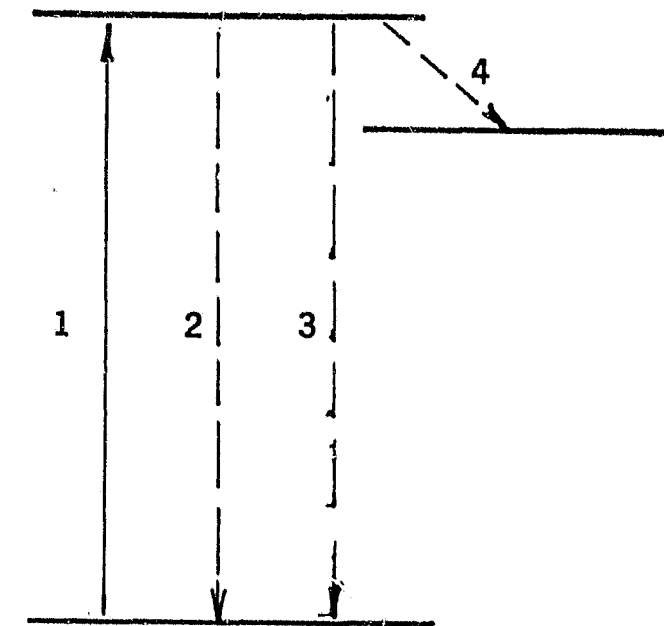
LIST OF FIGURES

<u>FIGURE</u>	<u>TITLE</u>
1	Molecular Processes in Optoacoustic Spectroscopy
2	Variation of Optoacoustic Signal with Incident Power
3	Block Diagram of Apparatus Used in Study
4	Test for Linearity Using 20 CO ₂ Laser Lines
5	Schematic Representation of Spectral Distribution of Absorptions of Explosives and Interfering Species
6	Vapor Pressure of Explosives
7	Optoacoustic Spectrum of NG at 6 Microns (45°C)
8	Optoacoustic Spectrum of EGDN at 6 Microns (45°C)
9	Optoacoustic Spectrum of DNT at 6 Microns (45°C)
10	Optoacoustic Spectrum of TNT at 6 Microns (45°C)
11	Optoacoustic Spectrum of RDX at 6 Microns (45°C)
12	Optoacoustic Spectrum of PETN at 6 Microns (45°C)
13	Optoacoustic Spectrum of TOVEX at 6 Microns (45°C)
14	Optoacoustic Spectrum of Dynamite at 6 Microns (45°C)
15	Optoacoustic Spectrum of NG at 9 Microns (45°C)
16	Optoacoustic Spectrum of EGDN at 9 Microns (45°C)
17	Optoacoustic Spectrum of DNT at 9 Microns (45°C)
18	Optoacoustic Spectrum of Dynamite at 9 Microns (23°C)
19	Optoacoustic Spectrum of Black Powder at 9 Microns (23°C)
20	Optoacoustic Spectrum of NG at 11 Microns (23°C)
21	Optoacoustic Spectrum of NG at 11 Microns (45°C)
22	Optoacoustic Spectrum of EGDN at 11 Microns (23°C)
23	Optoacoustic Spectrum of EGDN at 11 Microns (45°C)

<u>Figure</u>	<u>Title</u>
24	Optoacoustic Spectrum of Butane at 6 Microns
25	Optoacoustic Spectrum of Methane at 6 Microns
26	Optoacoustic Spectrum of NO ₂ at 6 Microns
27	Optoacoustic Spectrum of NO at 6 Microns
28	Optoacoustic Spectrum of Water Vapor at 6 Microns
29	Optoacoustic Spectrum of Butane at 9 Microns
30	Comparison EGDN and Water Vapor Optoacoustic Spectra at 6 Microns (50% Relative Humidity)
31	Comparison of NG and Water Vapor Optoacoustic Spectra at 6 Microns (20% Relative Humidity)
32	Comparison of NG and Water Vapor Optoacoustic Spectra at 6 Microns (50% Relative Humidity)
33a	Optoacoustic Equipment Used In The Laboratory
33b	Optoacoustic Equipment Used In Field Trial
34	Optoacoustic Detection of SF ₆ in the 10.6 Micron Wavelength Region
A1	Low Resolution Absorption Spectrum of NG
A2	Low Resolution Absorption Spectrum of EGDN
A3	Low Resolution Absorption Spectra of 2,3 DNT, 2,4, DNT, 2,6 DNT, and 3,4 DNT
A4	Low Resolution Absorption Spectrum of TNT
A5	Low Resolution Absorption Spectrum of RDX
A6	Low Resolution Absorption Spectrum of PETN
A7	Low Resolution Absorption Spectrum of n-butane and Iso-butane

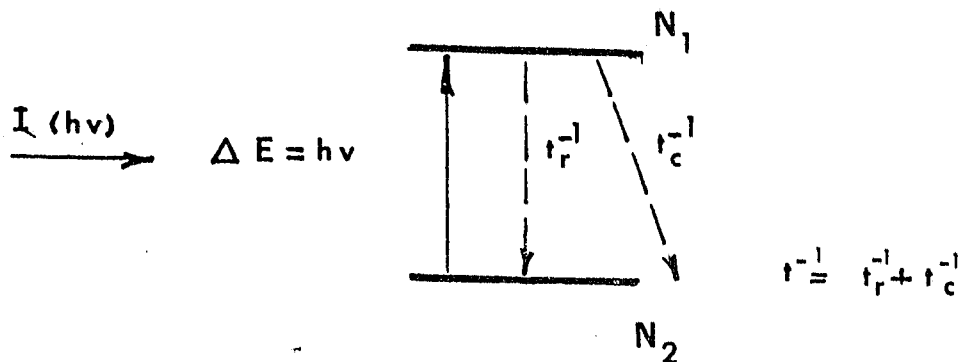
FigureTitle

- A8 Low Resolution Absorption Spectrum of Water Vapor
 A9 High Resolution Absorption Spectrum of NO
 A10 High Resolution Absorption Spectrum of NO₂
 A11 Low Resolution Absorption Spectrum of Methane



1. INCIDENT RADIATION ABSORBED
MOLECULE EXCITED VIBRATIONALLY
2. FLUORESCENCE
3. V-T ENERGY TRANSFER
4. INTERNAL ENERGY TRAPPING

FIGURE 1. MOLECULAR PROCESSES IN OPTOACOUSTIC SPECTROSCOPY



OPTOACOUSTIC SIGNAL $\propto \frac{B N I t_c^{-1}}{2(BI + t^{-1})^2}$

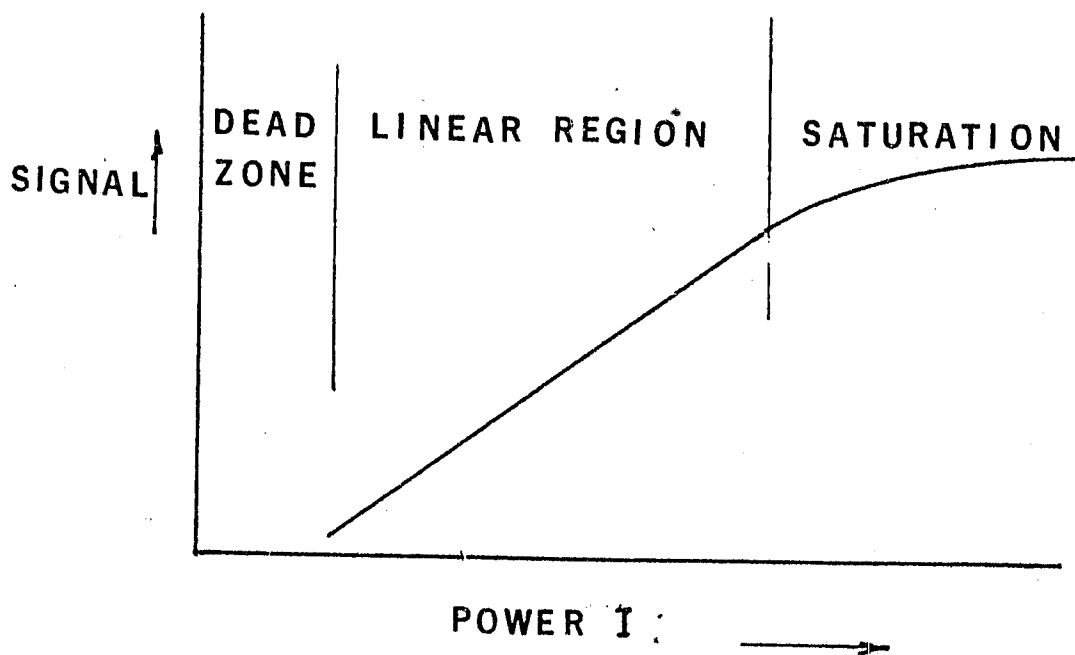
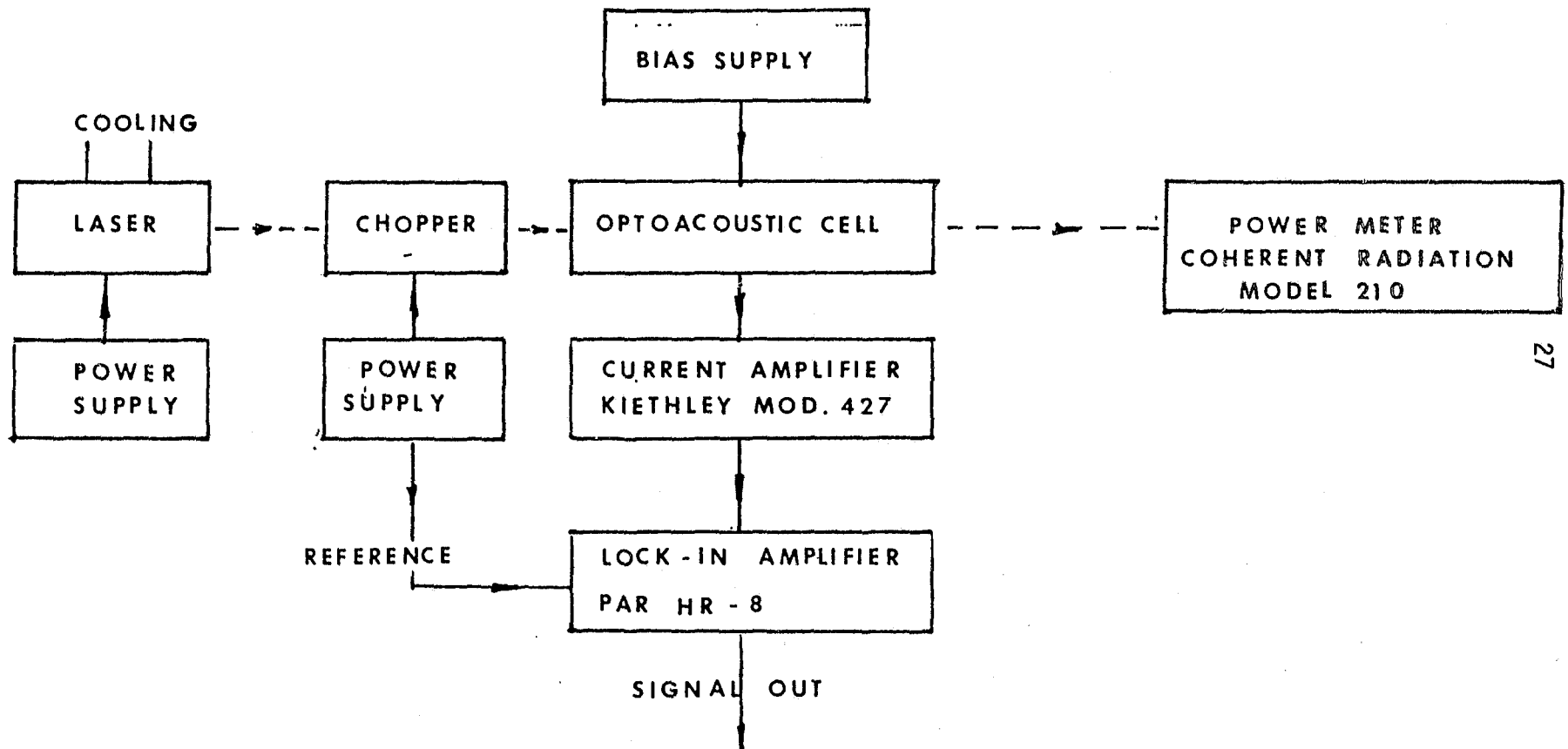


FIGURE 2. VARIATION OF OPTOACOUSTIC SIGNAL WITH INCIDENT POWER



27

FIGURE 3. BLOCK DIAGRAM OF APPARATUS USED IN STUDY

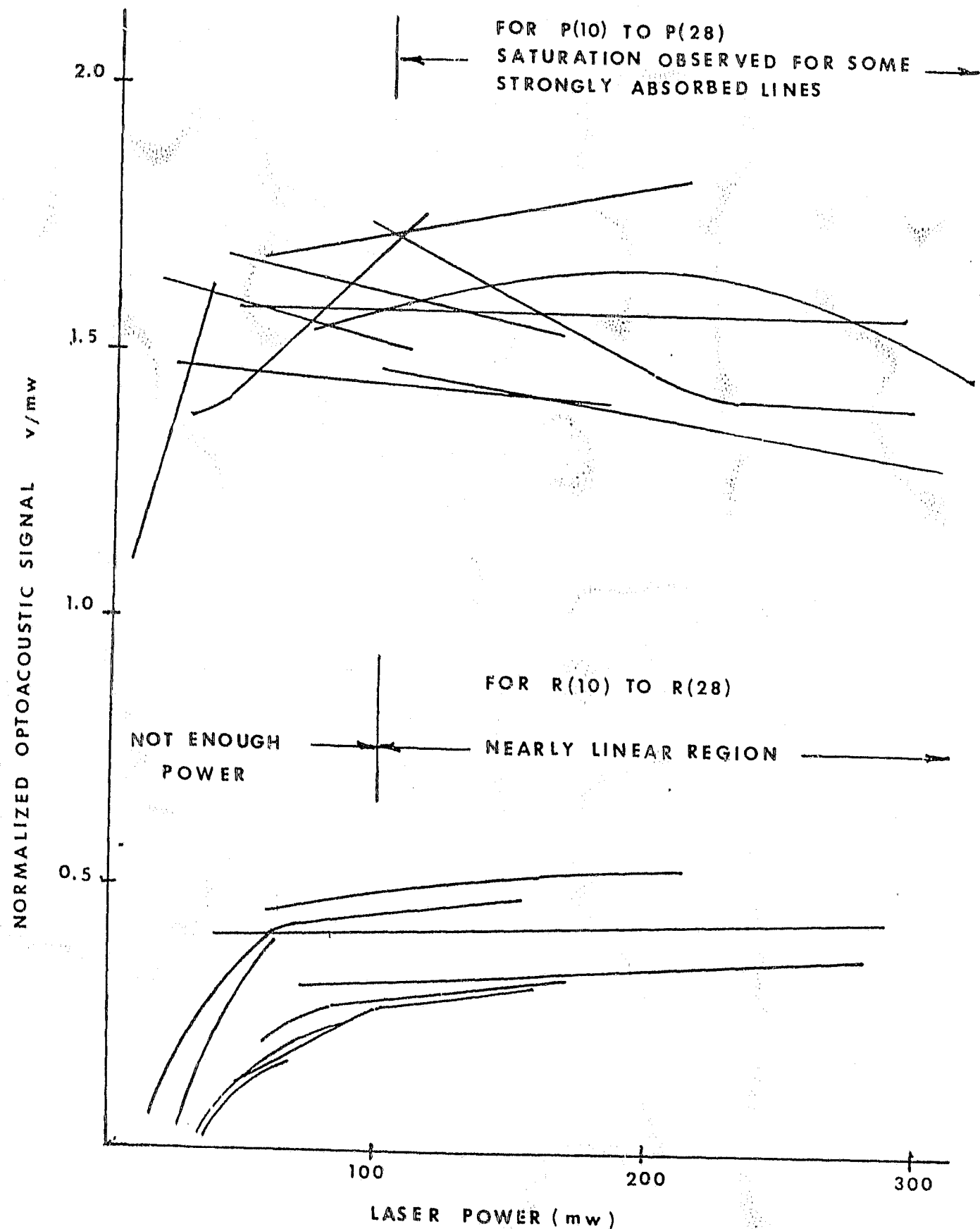


FIGURE 4. TEST FOR LINEARITY USING 20 CO₂ LASER LINES

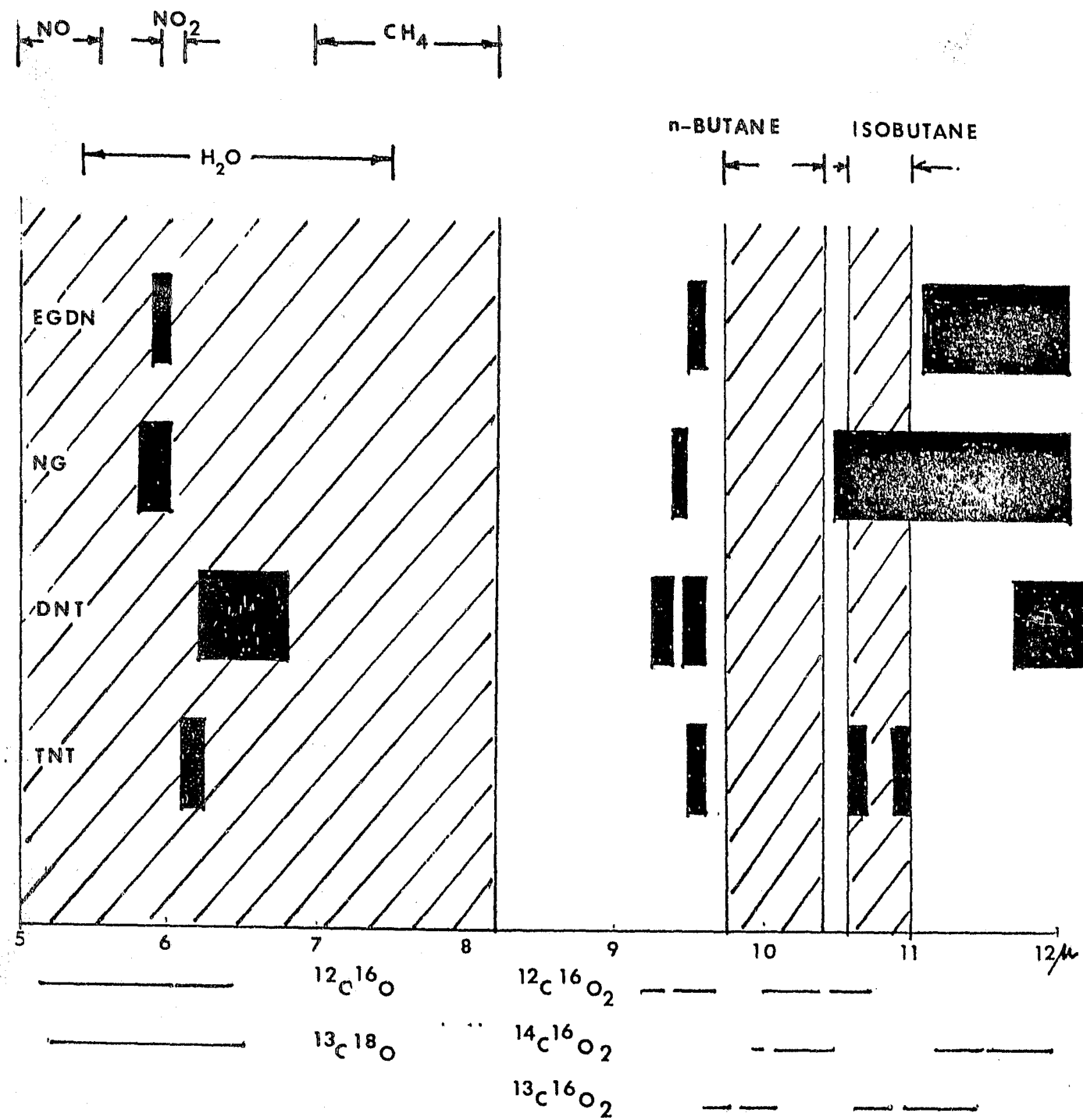


FIGURE 5. SCHEMATIC REPRESENTATION OF SPECTRAL DISTRIBUTION OF ABSORPTIONS OF EXPLOSIVES AND INTERFERING SPECIES

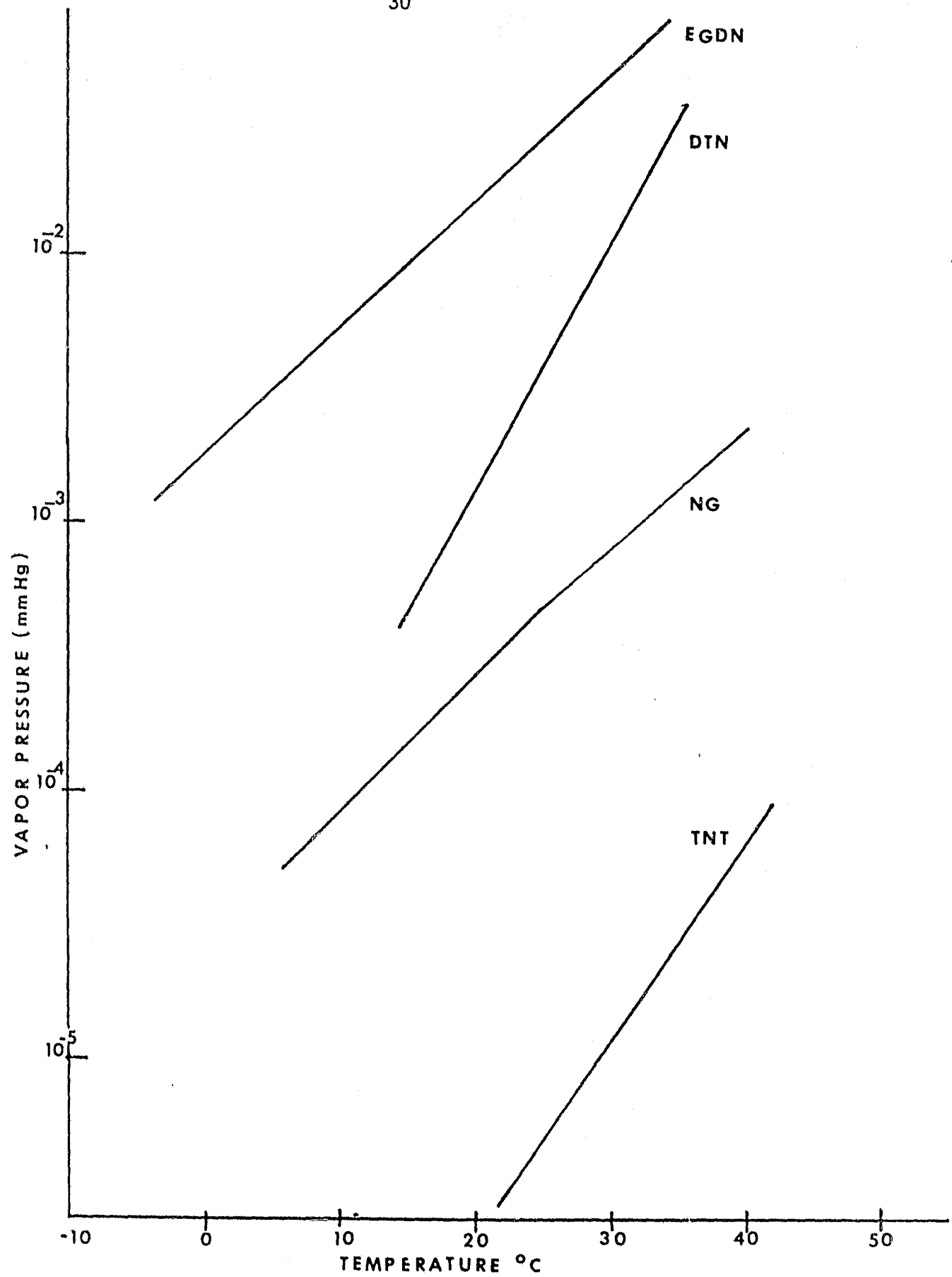


FIGURE 6. VAPOR PRESSURE OF EXPLOSIVES

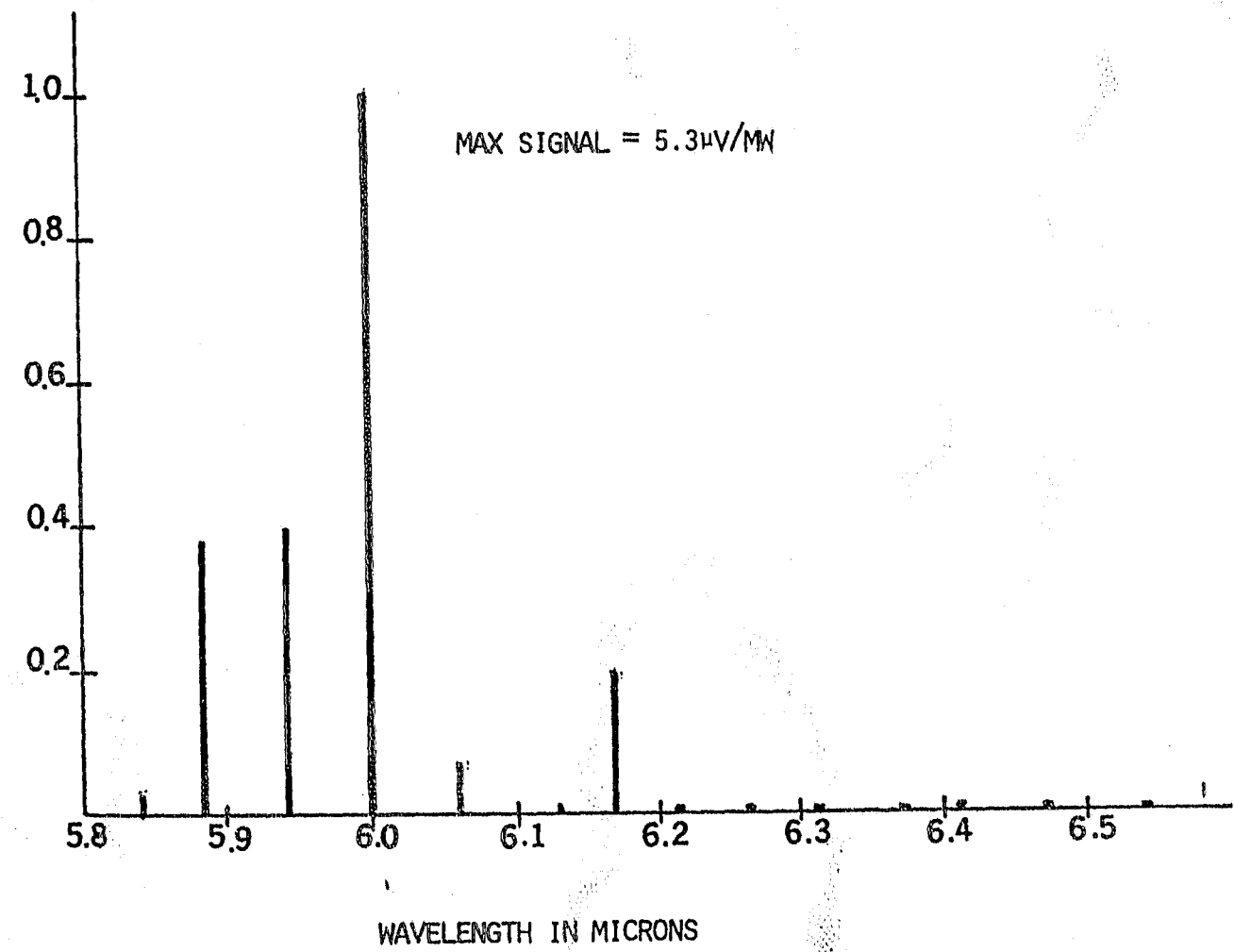


FIGURE 7. OPTOACOUSTIC SPECTRUM OF NG AT 6 MICRONS (45°C)

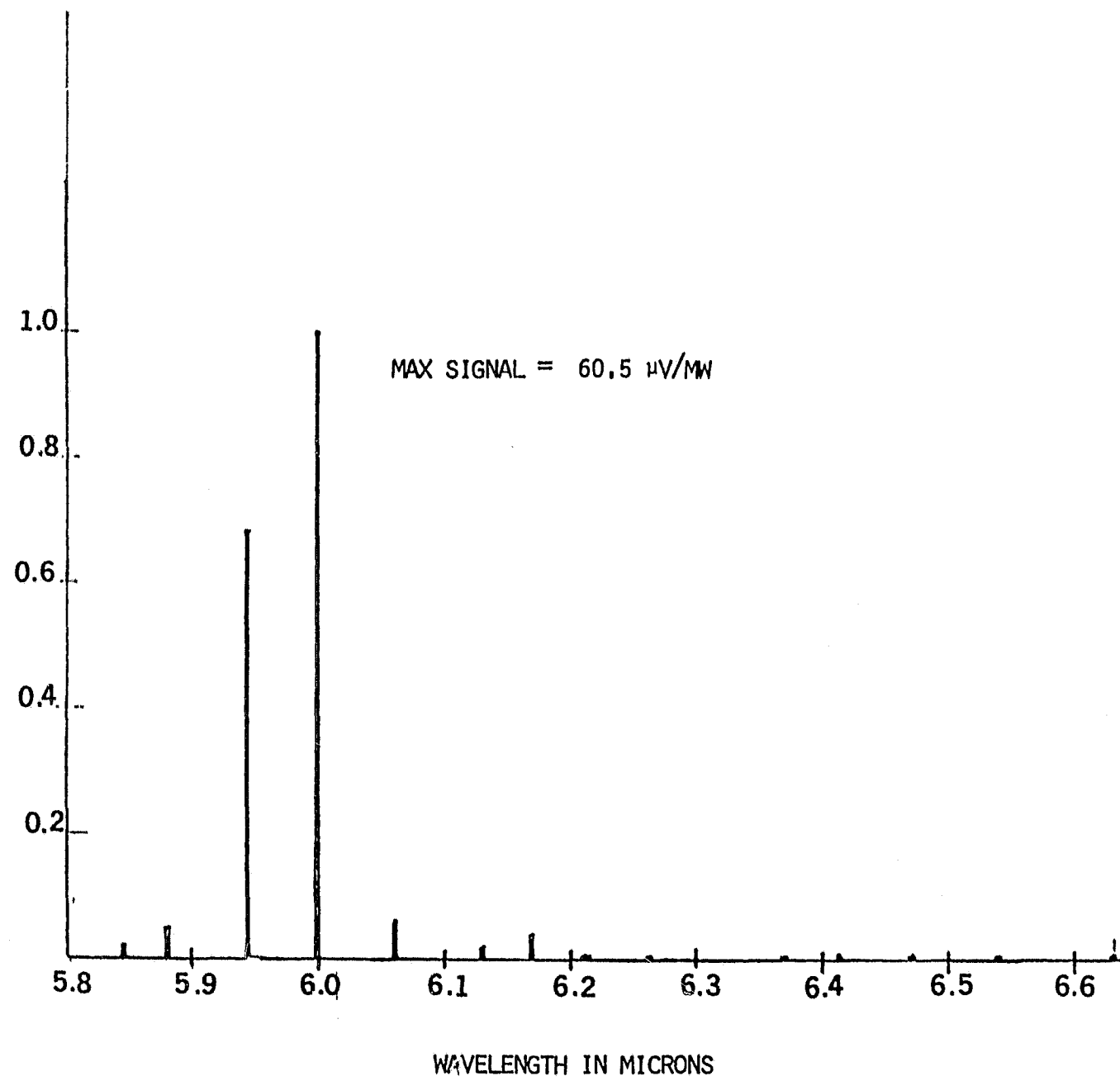


FIGURE 8. OPTOACOUSTIC SPECTRUM OF EGDN (10% NG) AT 6 MICRONS (45°C)

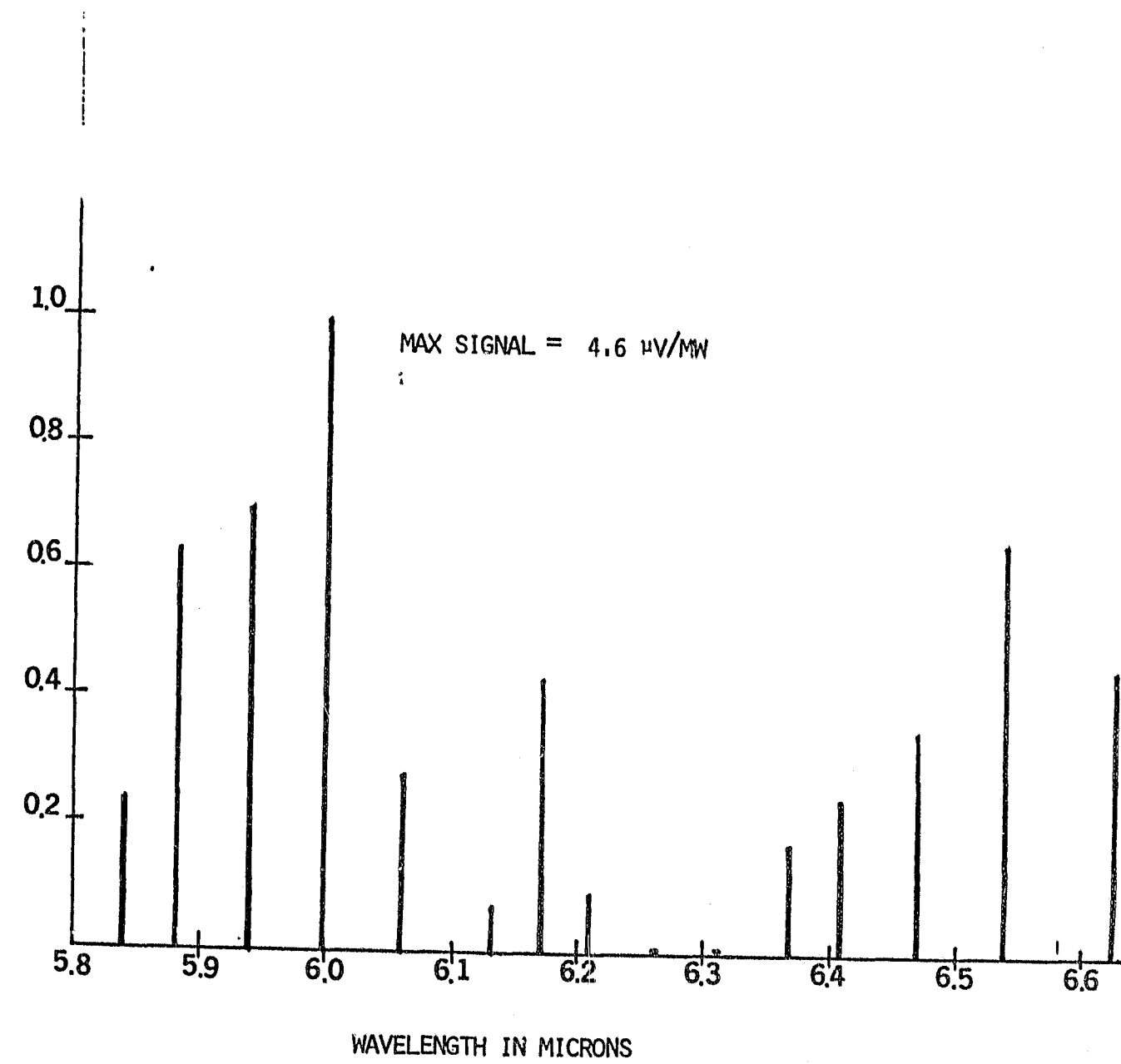


FIGURE 9. OPTOACOUSTIC SPECTRUM OF DNT AT 6 MICRONS (45°C)

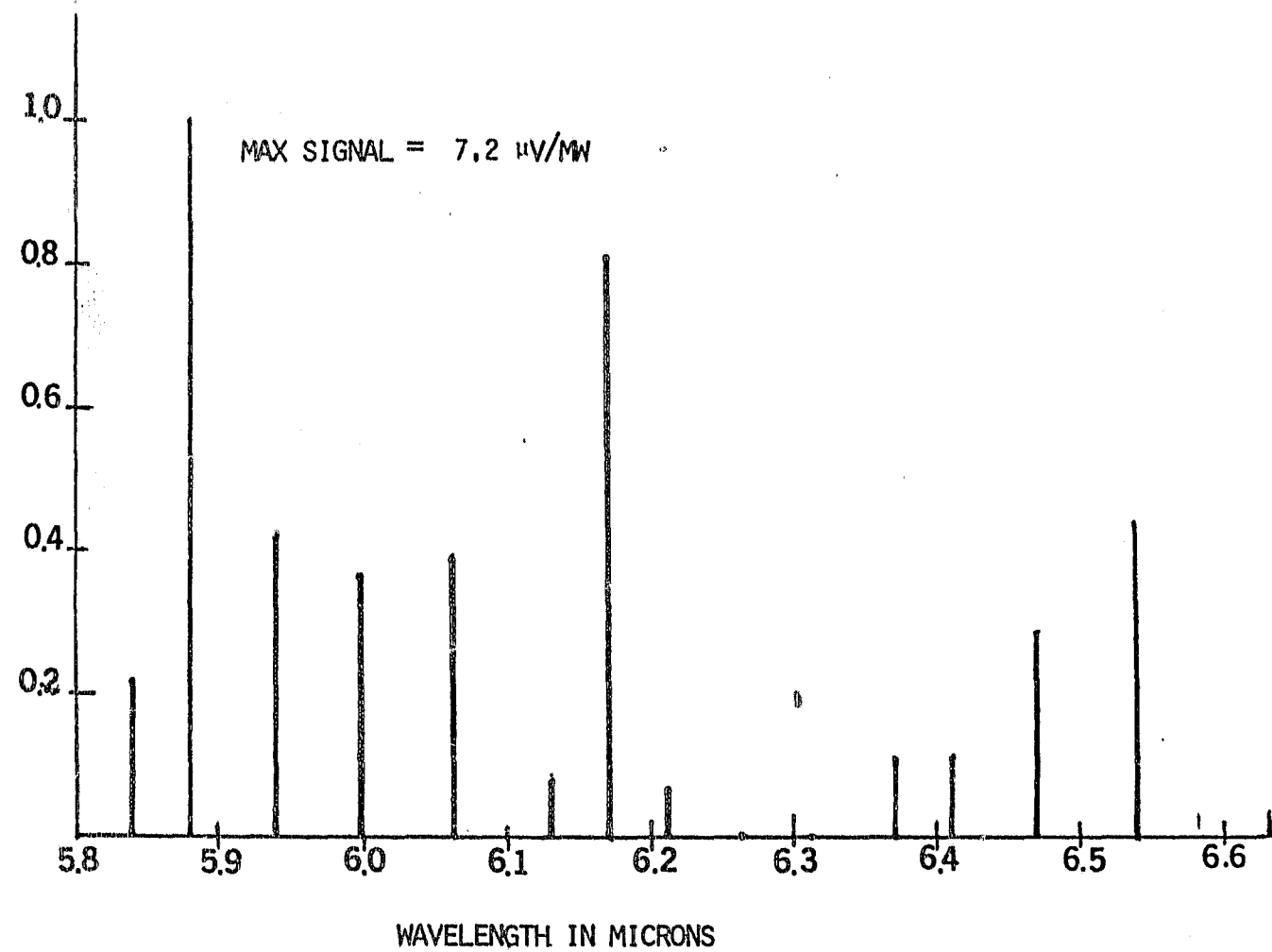


FIGURE 10. OPTOACOUSTIC SPECTRUM OF TNT AT 6 MICRONS (45°C)

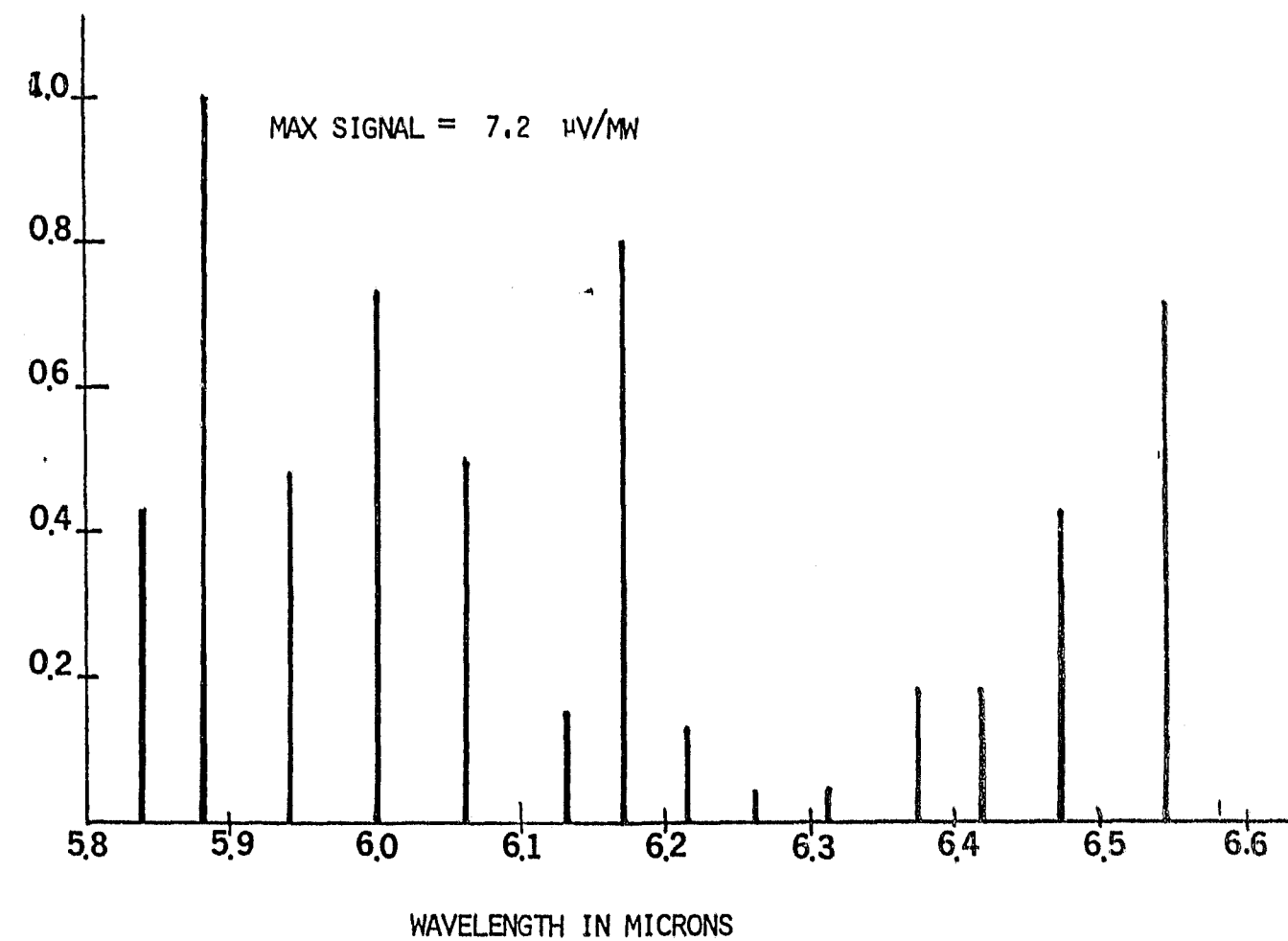


FIGURE 11. OPTOACOUSTIC SPECTRUM OF RDX AT 6 MICRONS (45°C)

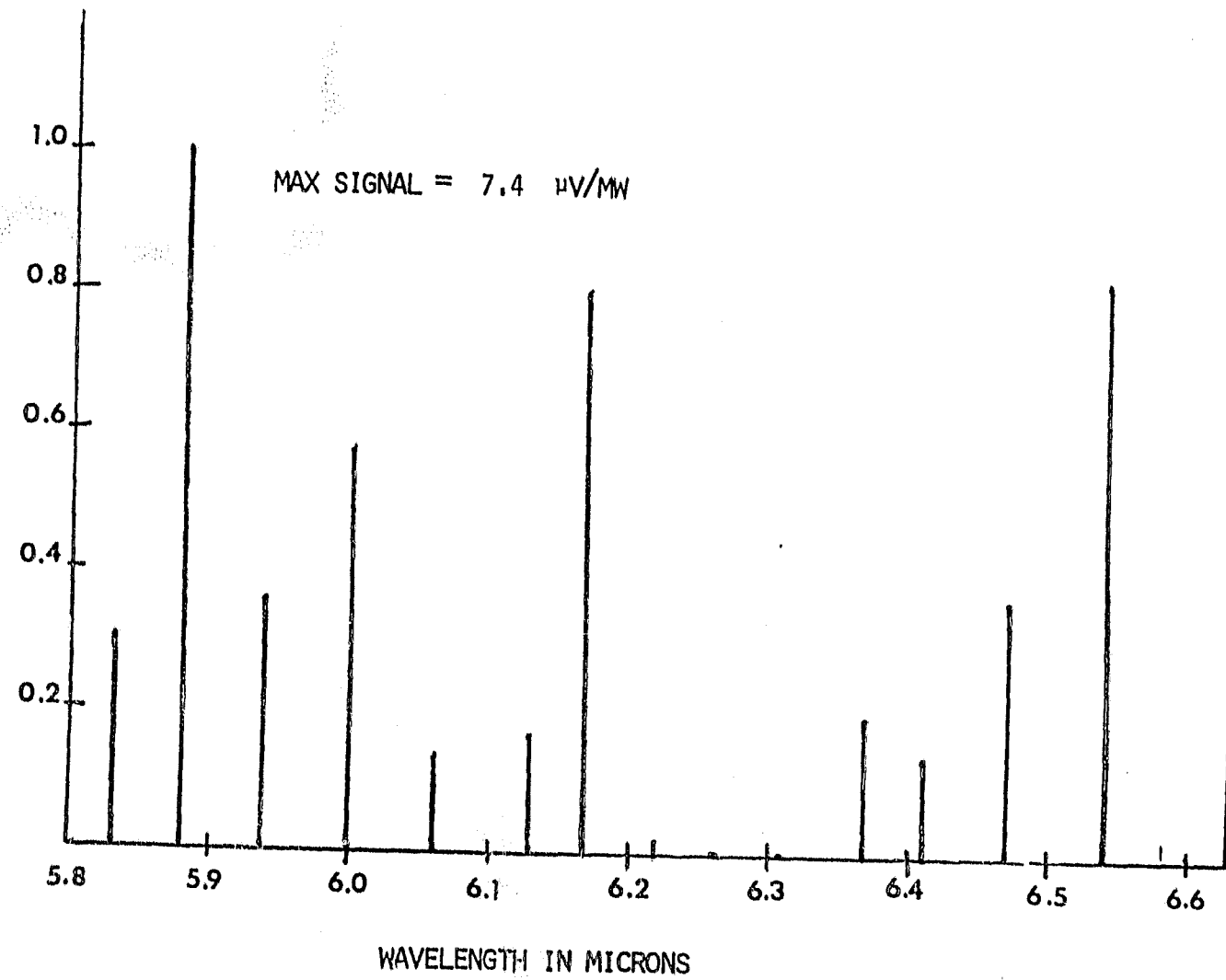


FIGURE 12. OPTOACOUSTIC SPECTRUM OF PETN AT 6 MICRONS (45°C)

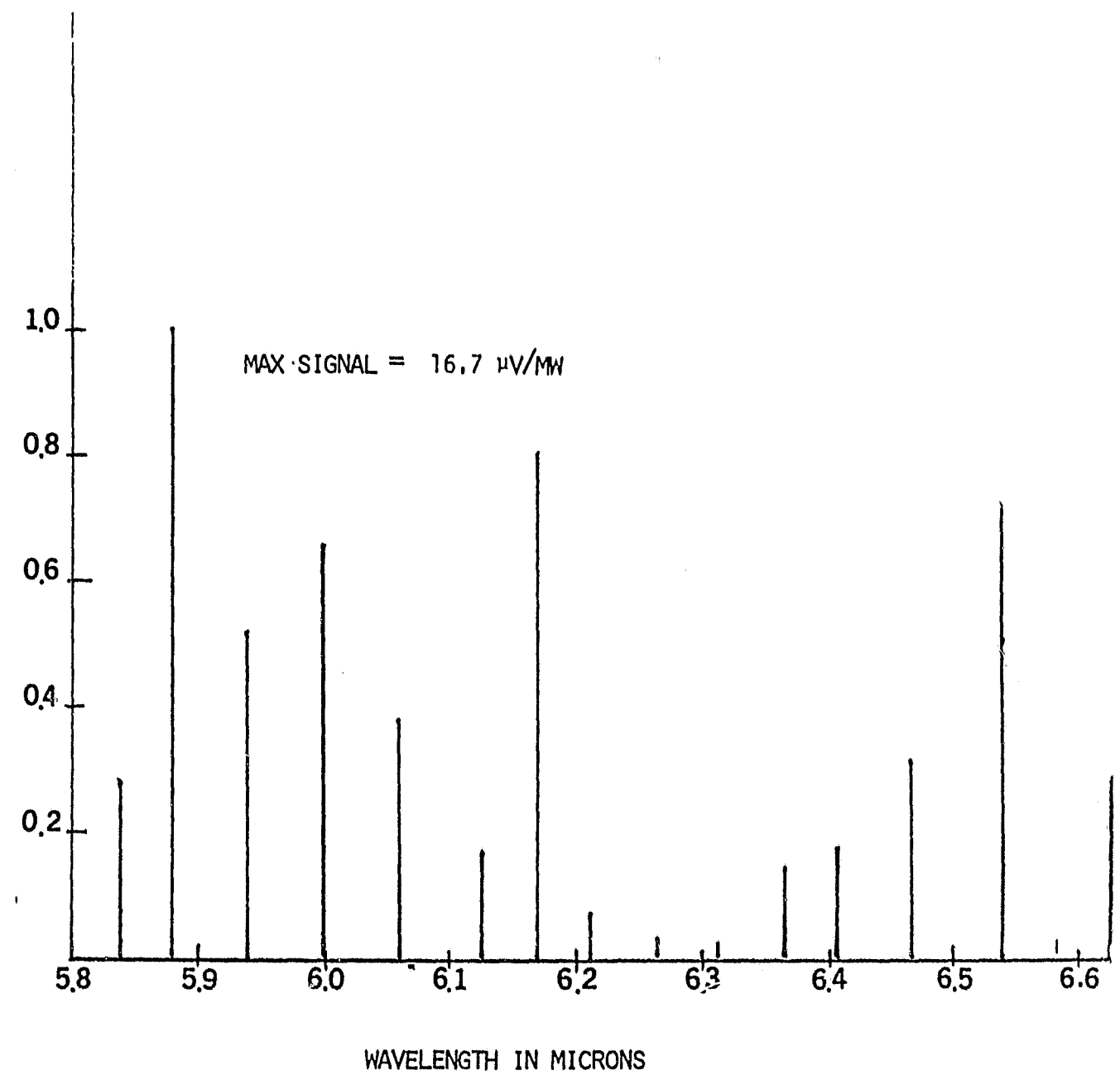


FIGURE 13. OPTOACOUSTIC SPECTRUM OF TOVEX AT 6 MICRONS (45°C)

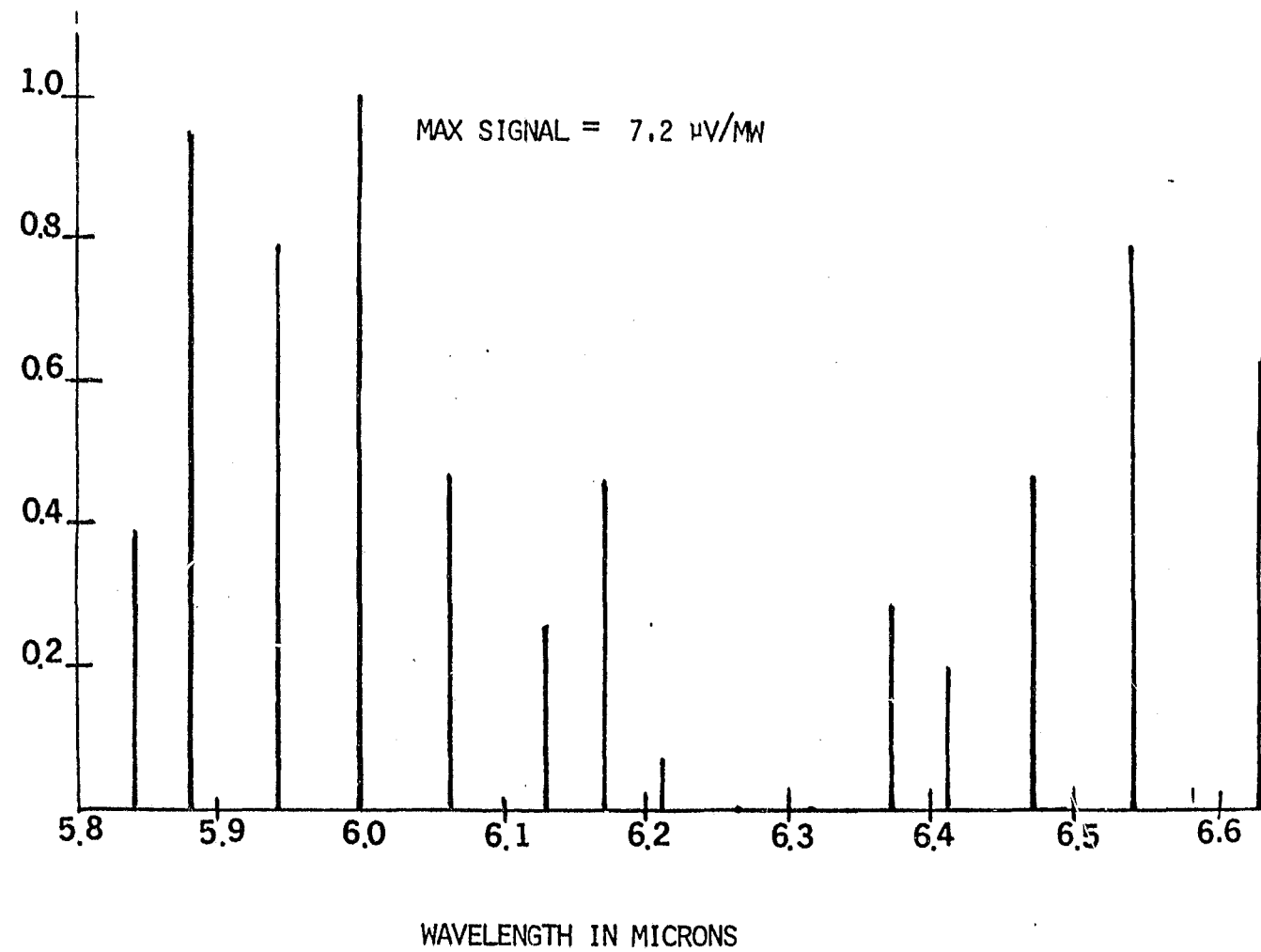


FIGURE 14. OPTOACOUSTIC SPECTRUM OF DYNAMITE AT 6 MICRONS (45°C)

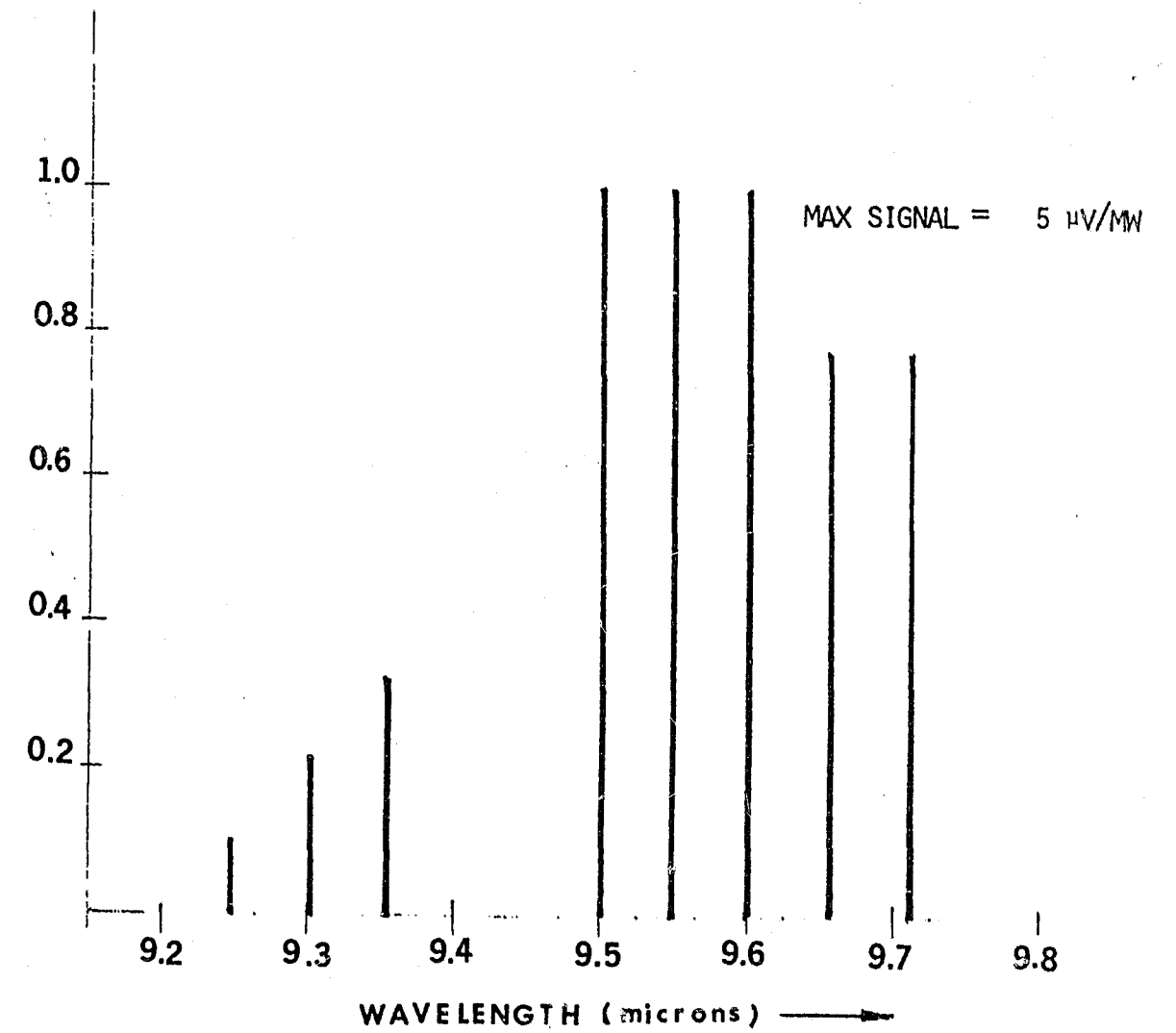


FIGURE 15. OPTOACOUSTIC SPECTRUM OF NG AT 9 MICRONS (45°C)

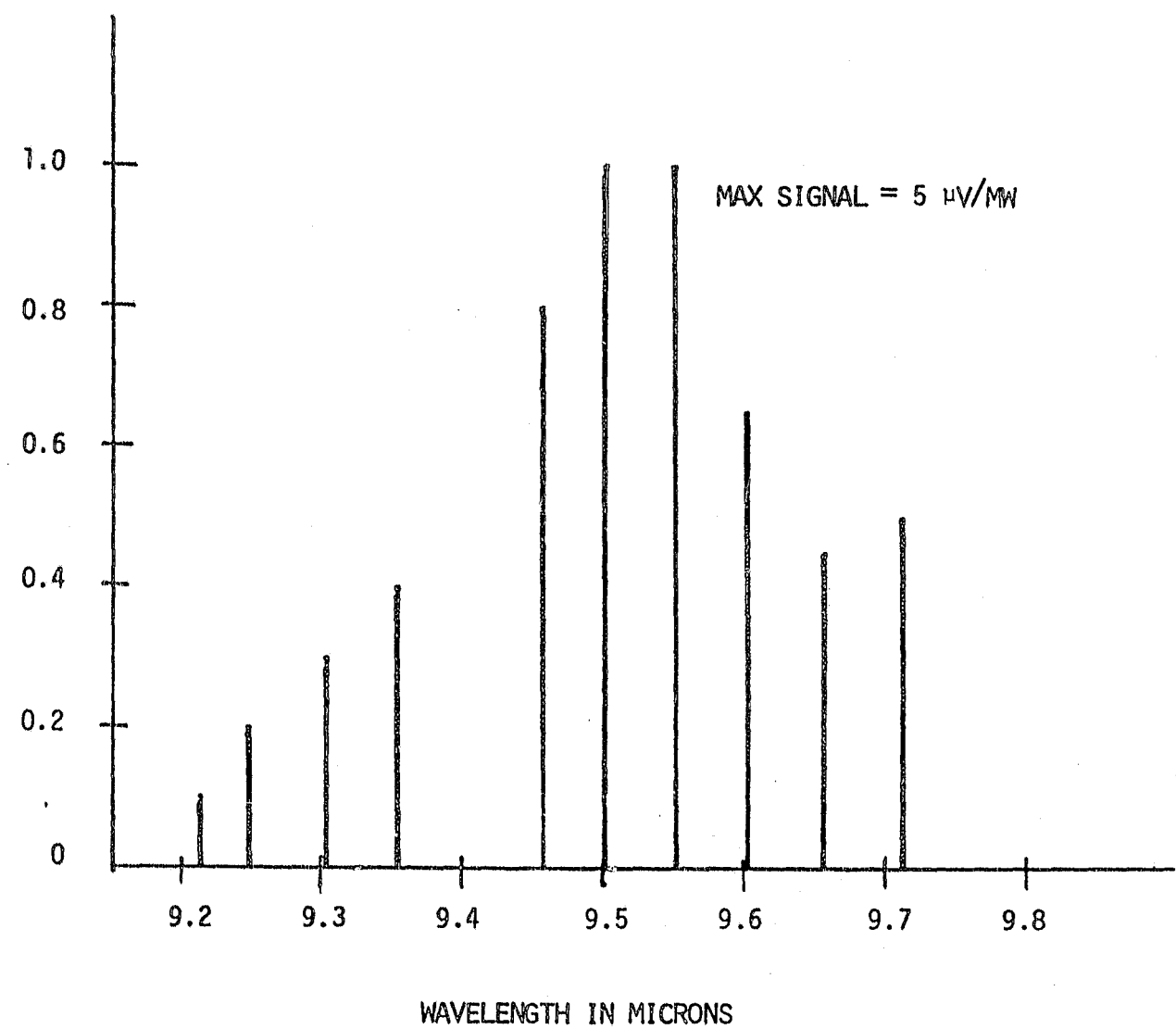


FIGURE 16. OPTOACOUSTIC SPECTRUM OF EGDN AT 9 MICRONS (45°C)

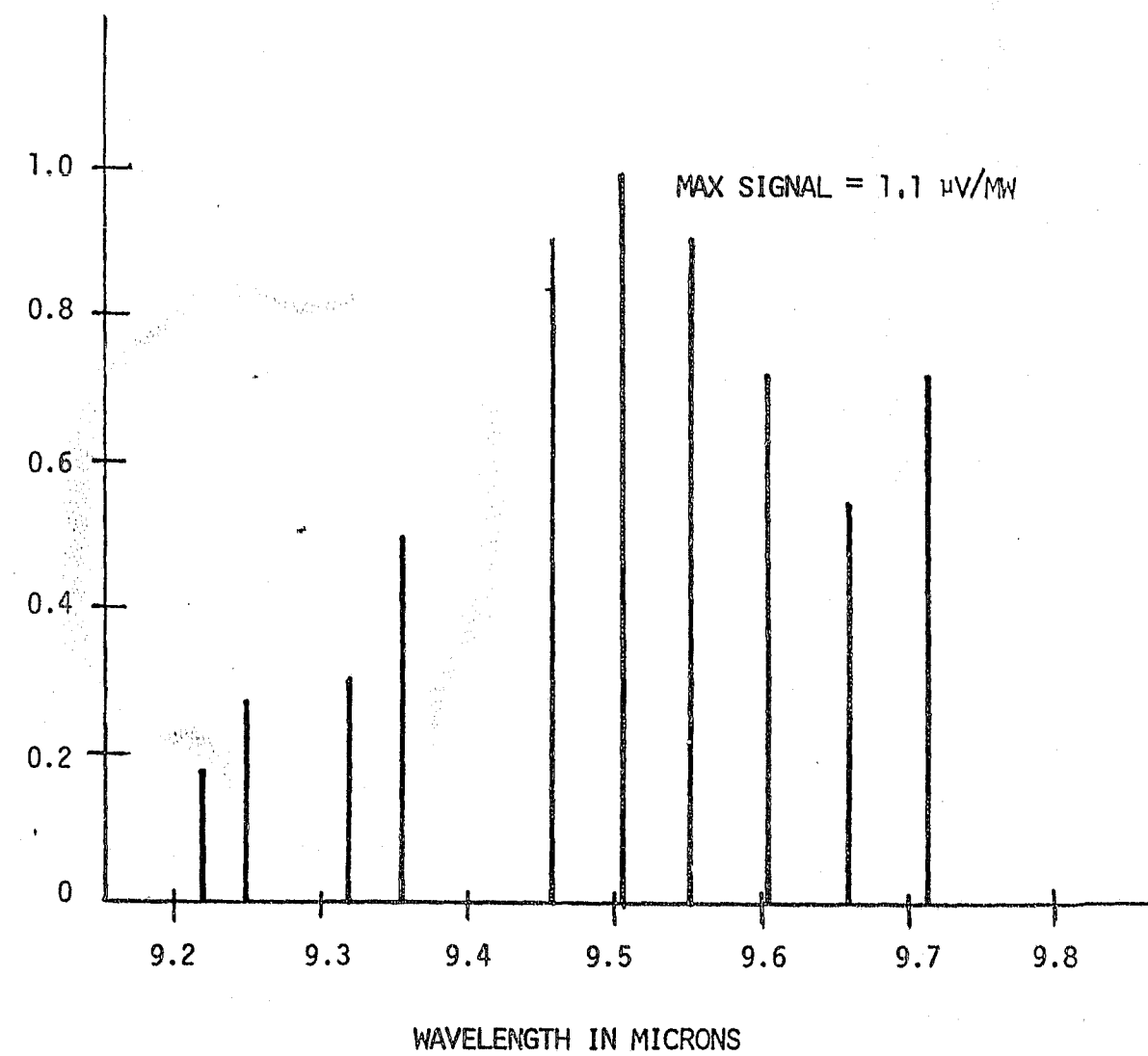


FIGURE 17. OPTOACOUSTIC SPECTRUM OF DNT AT 9 MICRONS (45°C)

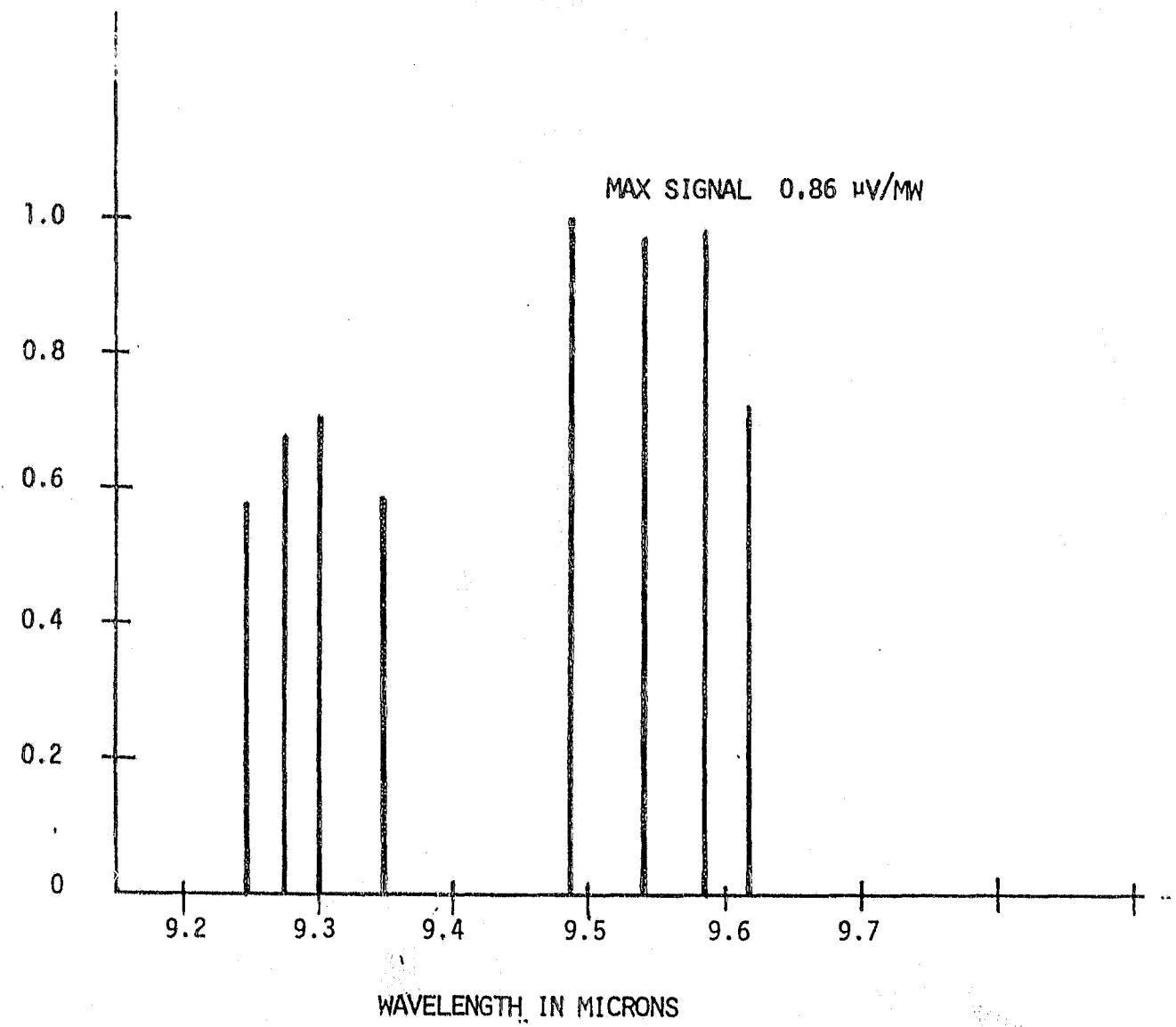


FIGURE 18. OPTOACOUSTIC SPECTRUM OF DYNAMITE AT 9 MICRONS (45°C)

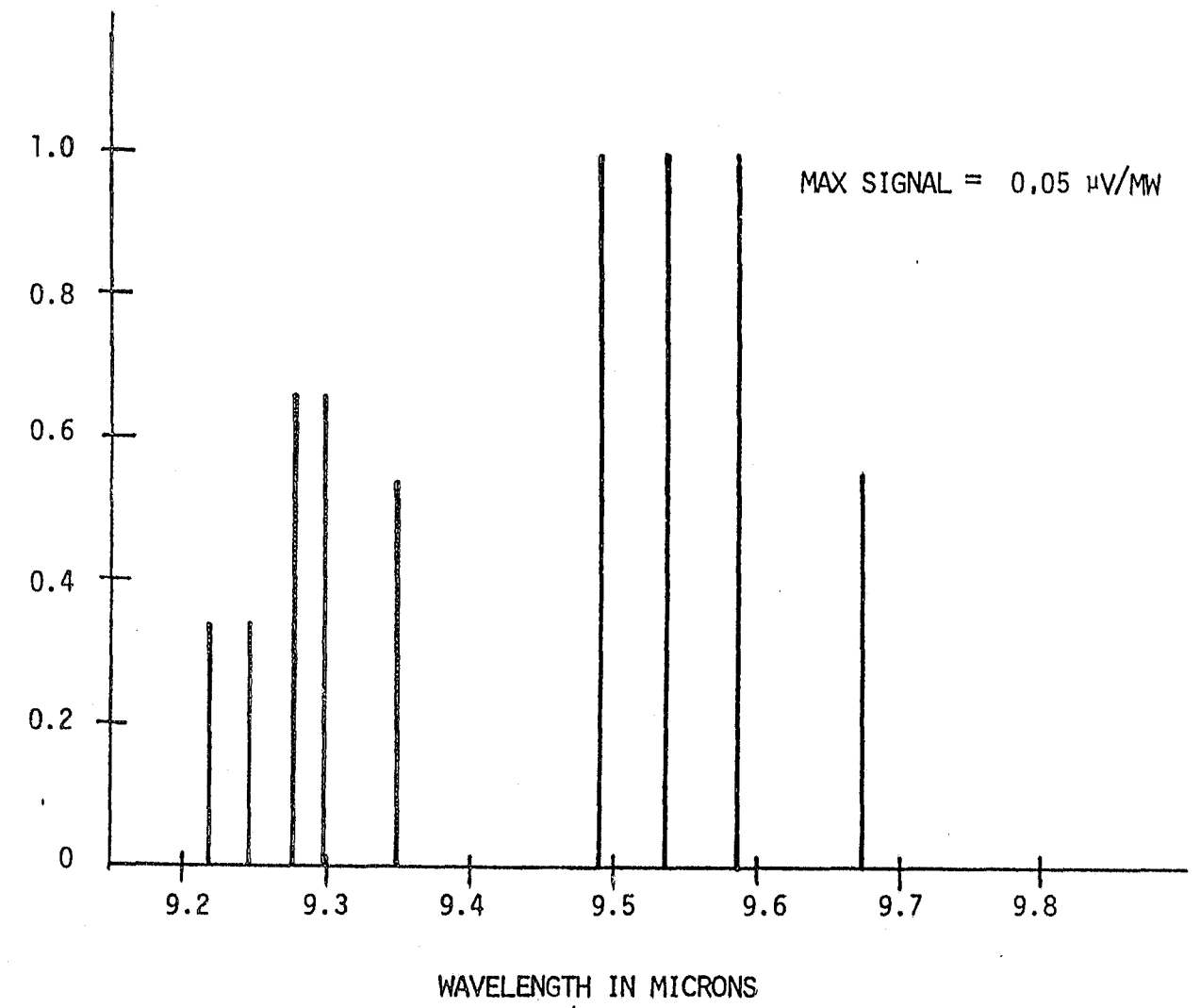


FIGURE 19. OPTOACOUSTIC SPECTRUM OF BLACK POWDER AT 9 MICRONS (45°C)

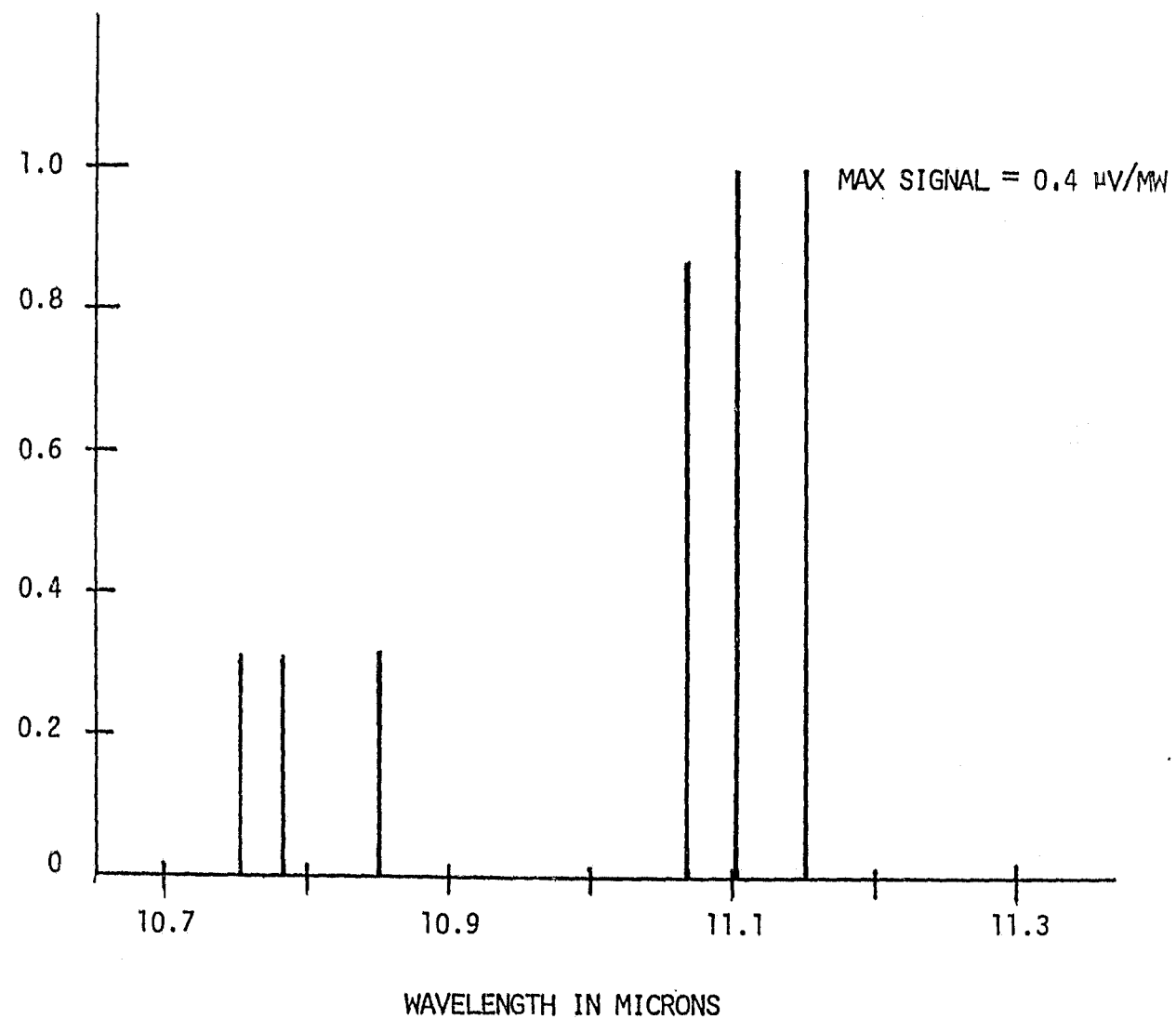


FIGURE 20. OPTOACOUSTIC SPECTRUM OF NG AT 11 MICRONS (23°C)

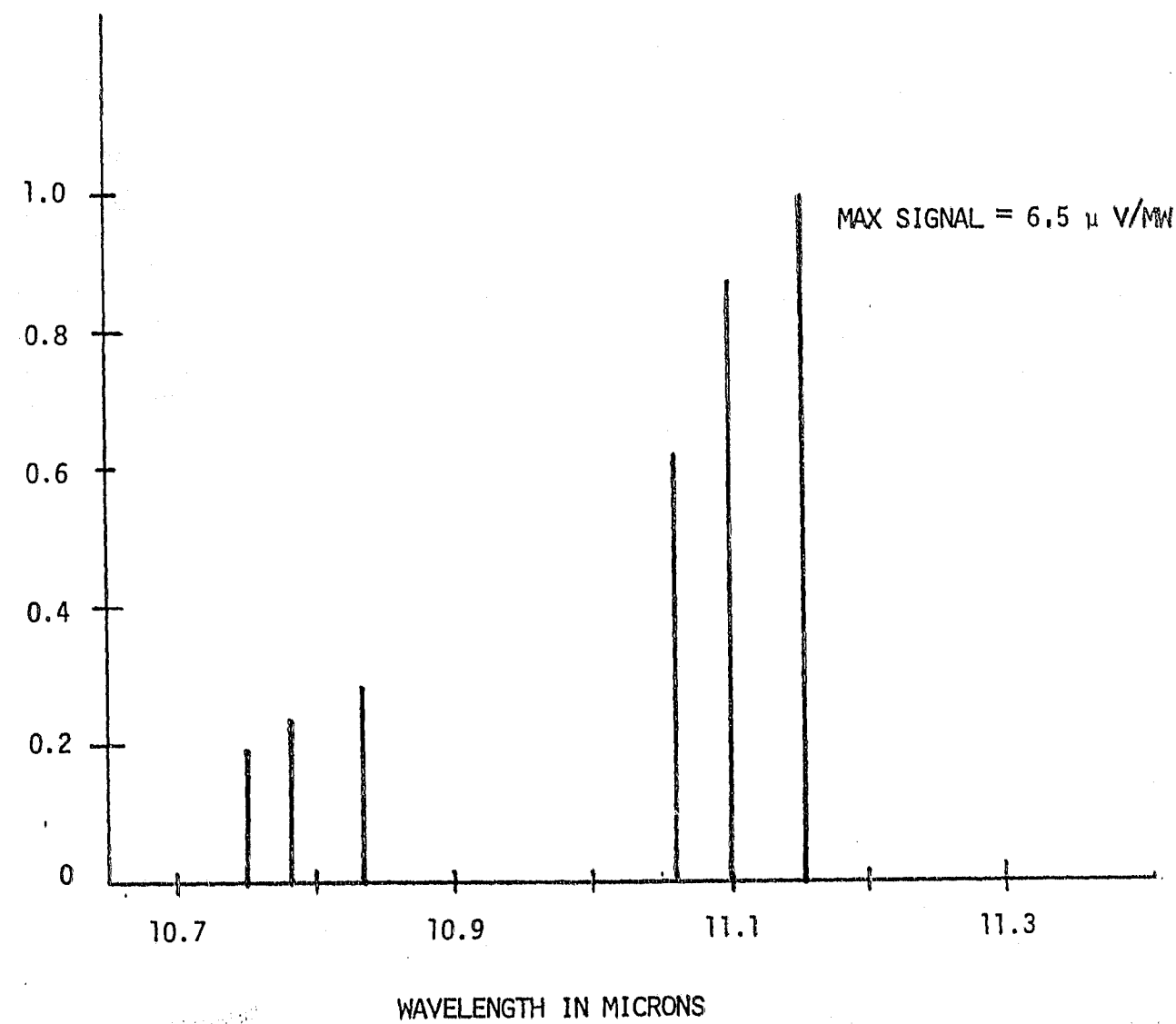


FIGURE 21. OPTOACOUSTIC SPECTRUM OF NG AT 11 MICRONS (45°C)

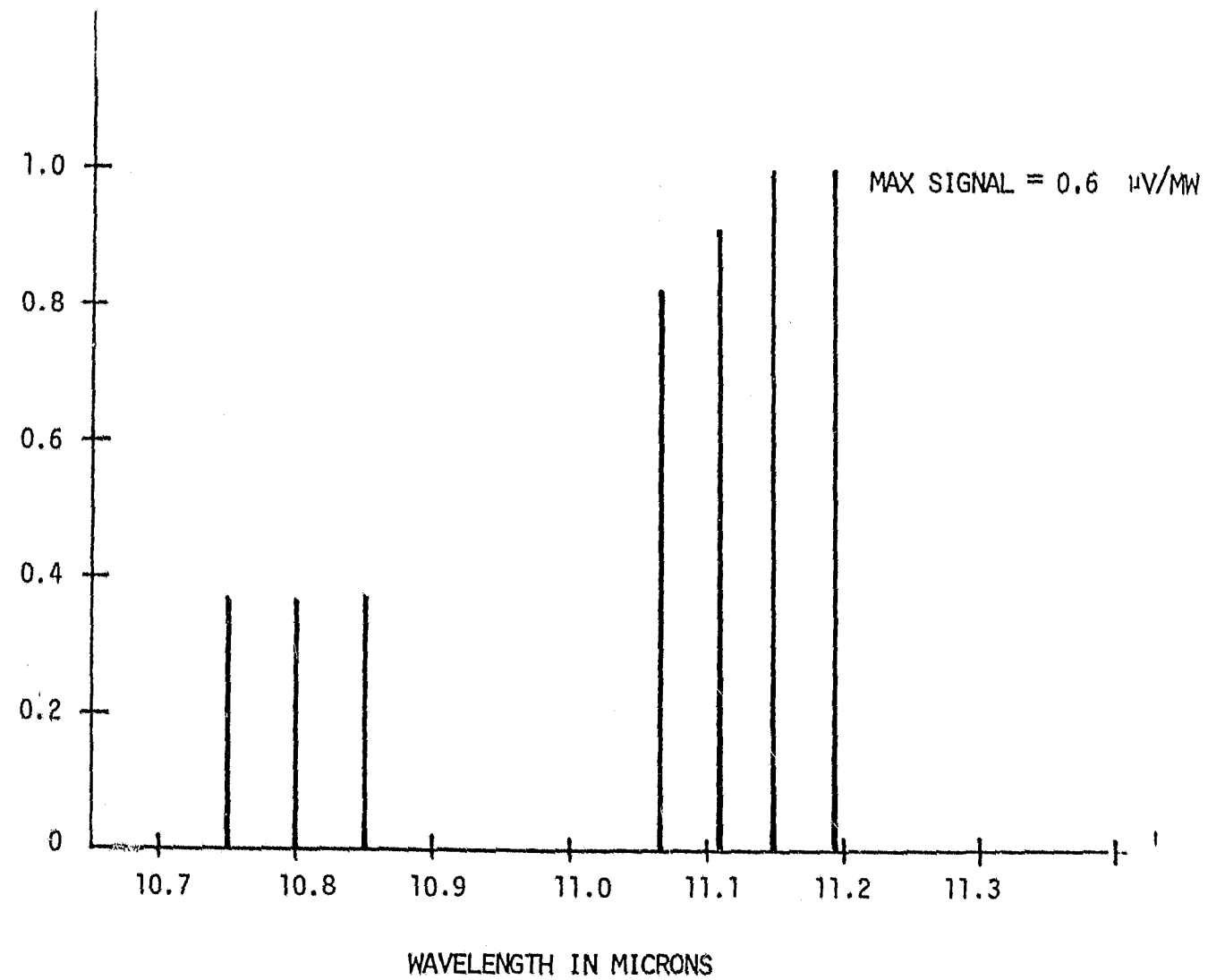


FIGURE 22. OPTOACOUSTIC SPECTRUM OF EGDN AT 11 MICRONS (23°C)

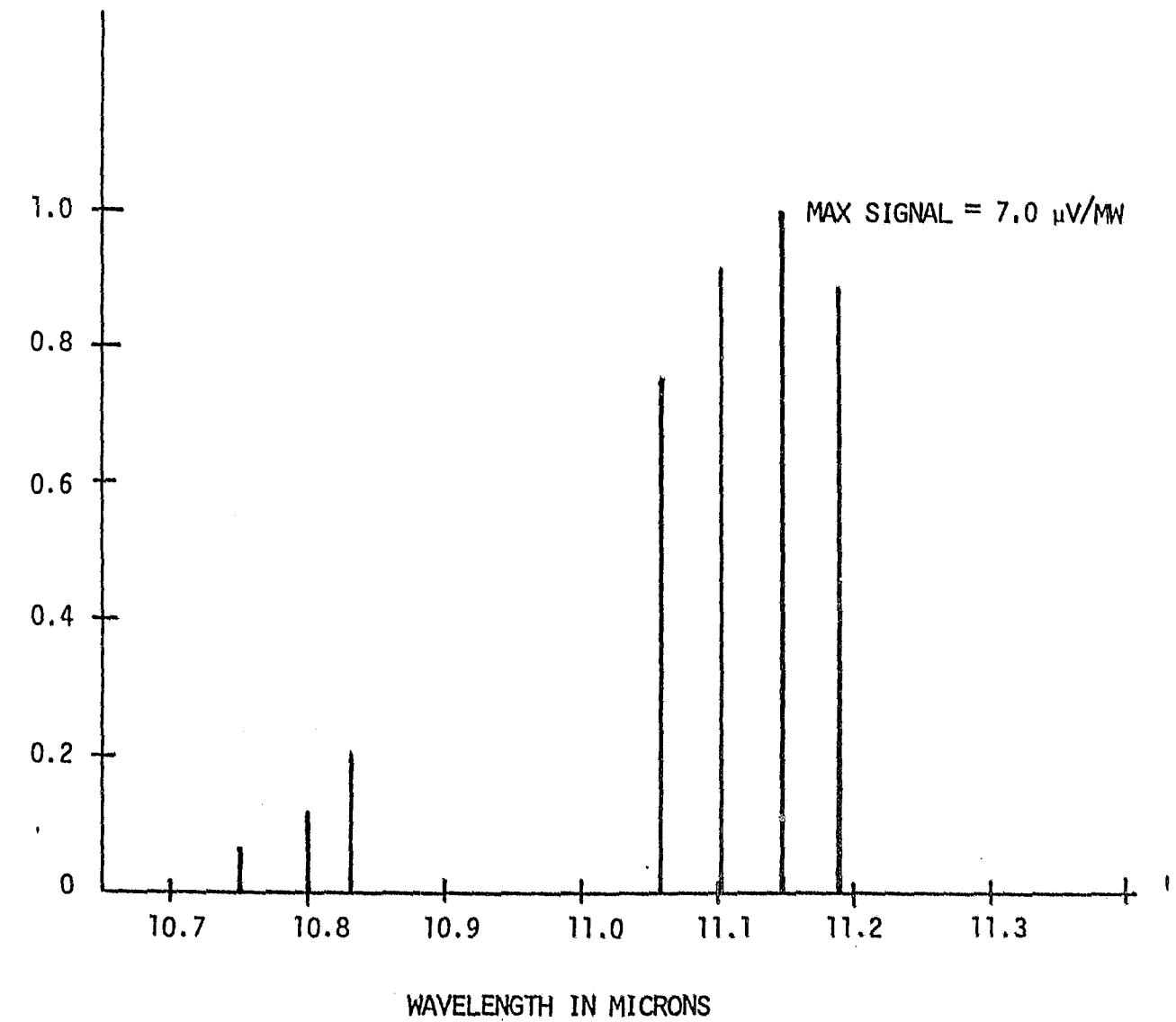


FIGURE 23. OPTOACOUSTIC SPECTRUM OF EGDN AT 11 MICRONS (45°C)

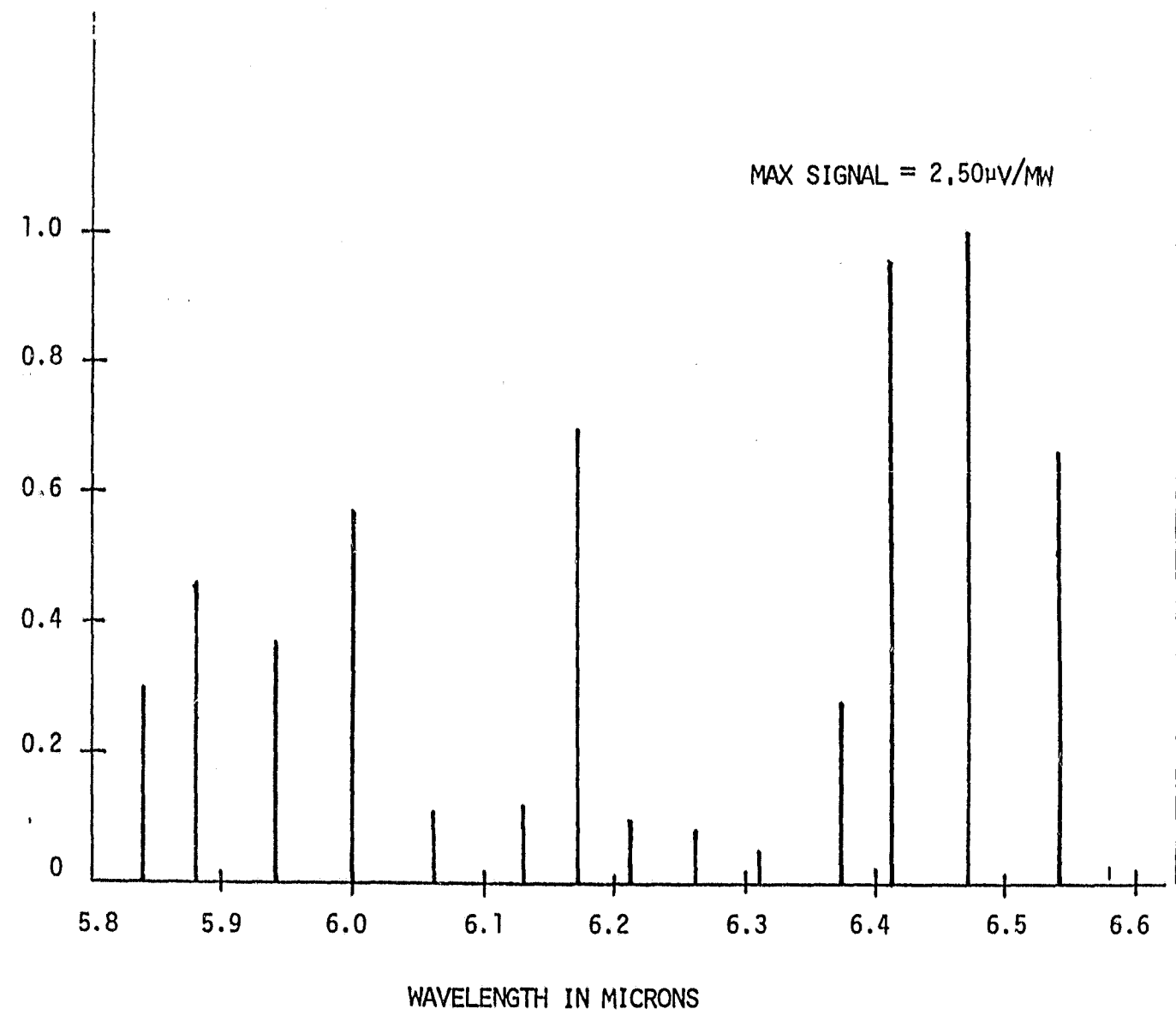


FIGURE 24. OPTOACOUSTIC SPECTRUM OF BUTANE AT 6 MICRONS

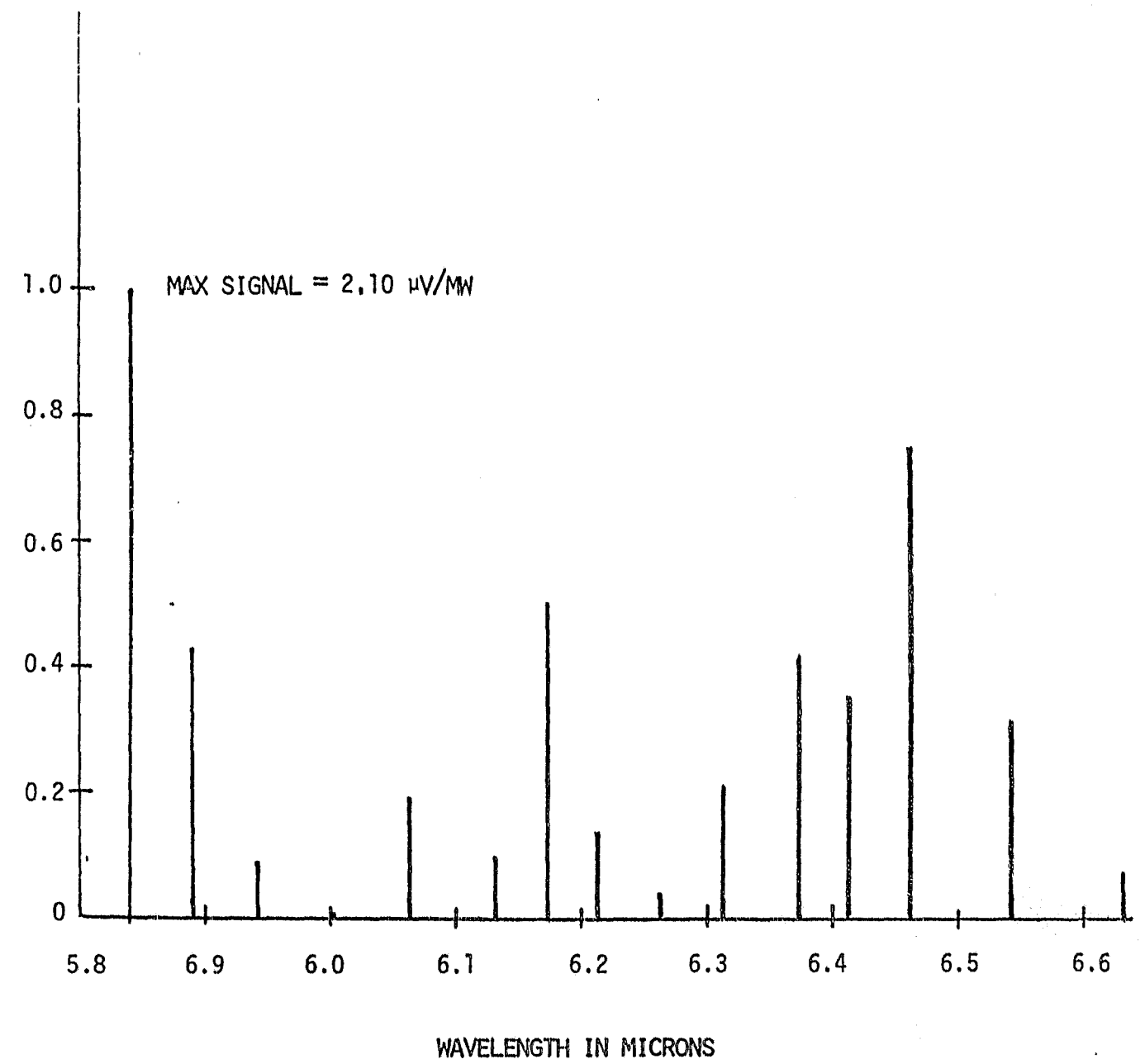


FIGURE 25. OPTOACOUSTIC SPECTRUM OF METHANE AT 6 MICRONS

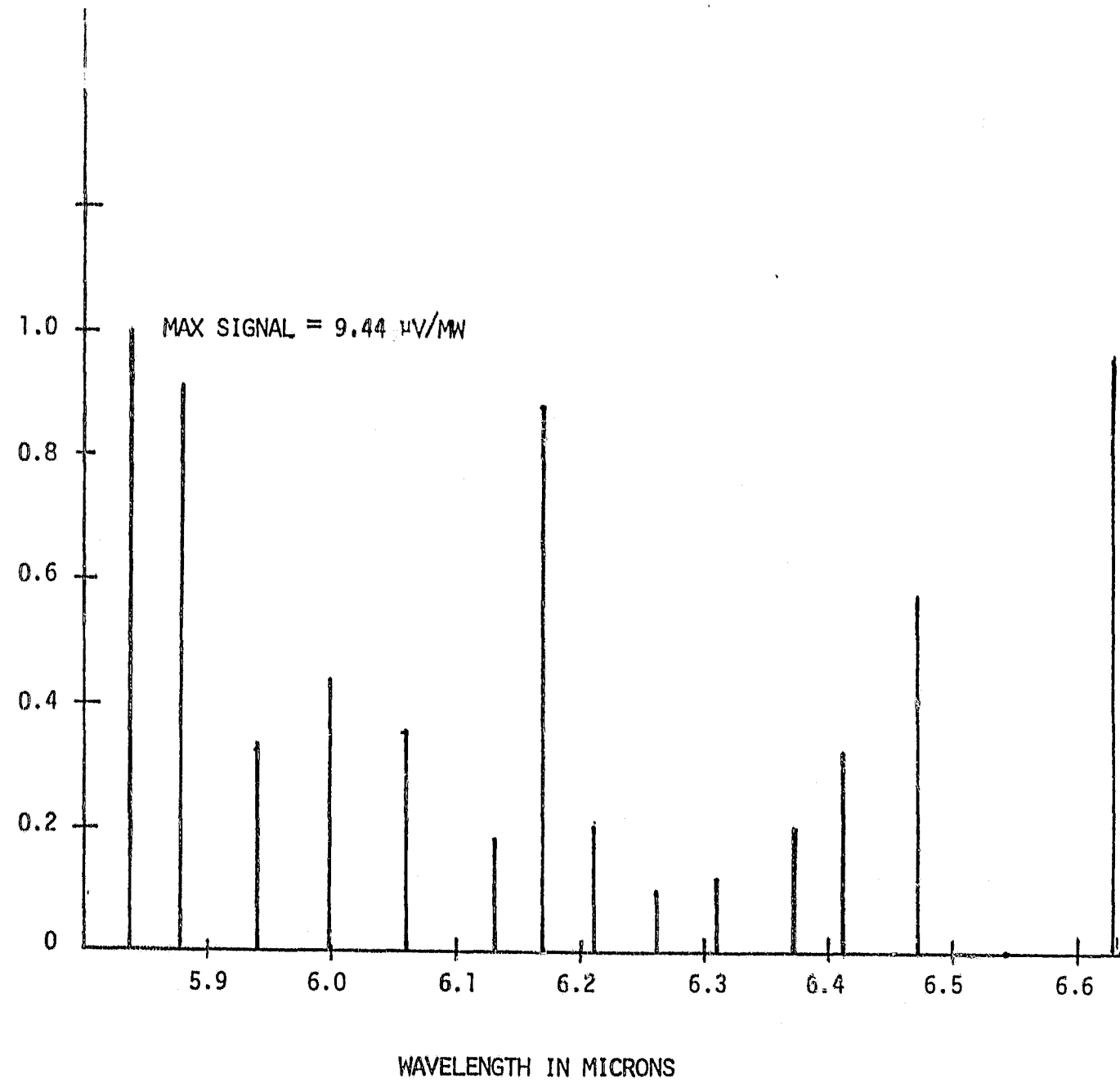


FIGURE 26. OPTOACOUSTIC SIGNAL OF NO_2 AT 6 MICRONS

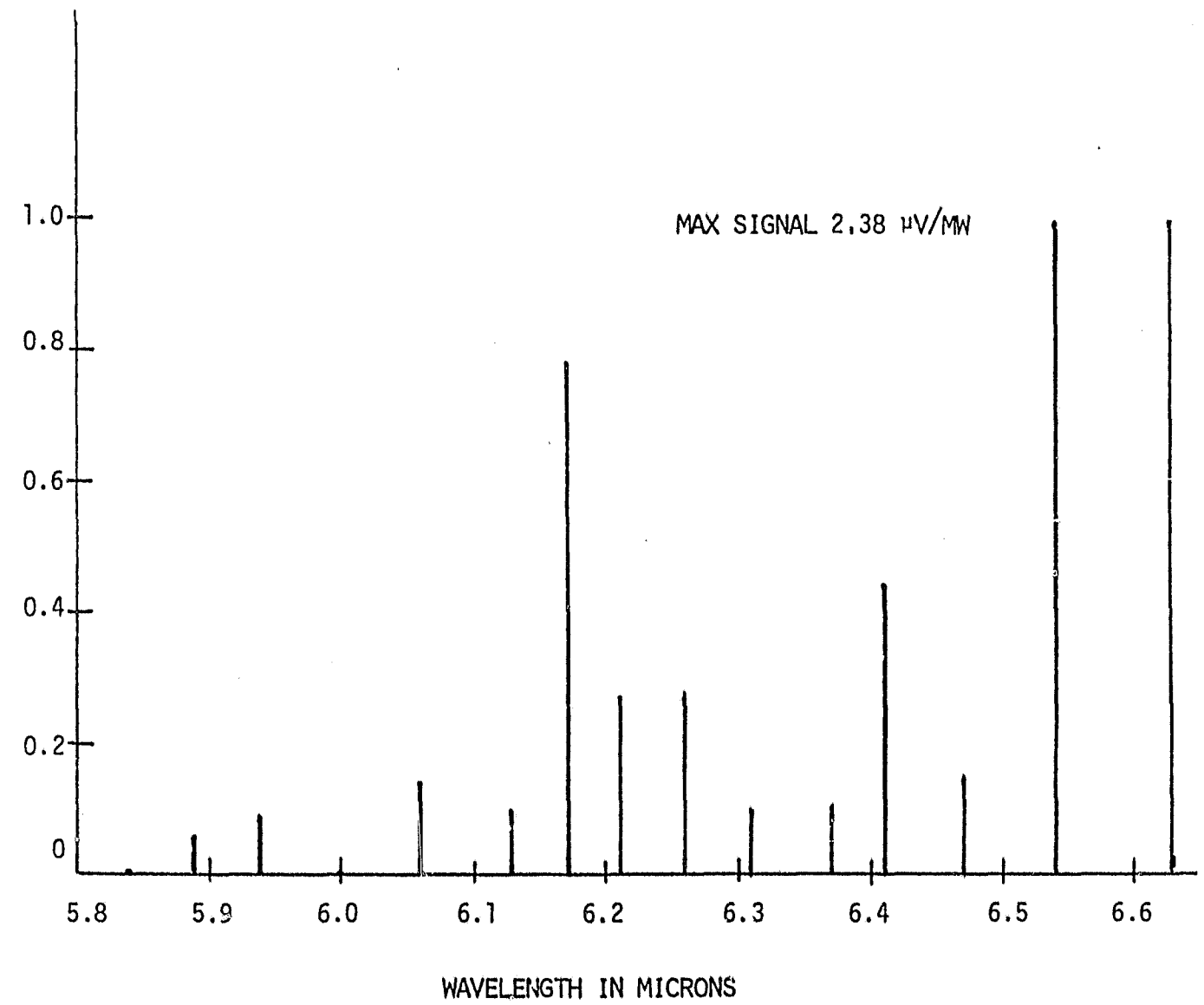


FIGURE 27. OPTOACOUSTIC SPECTRUM OF NO AT 6 MICRONS

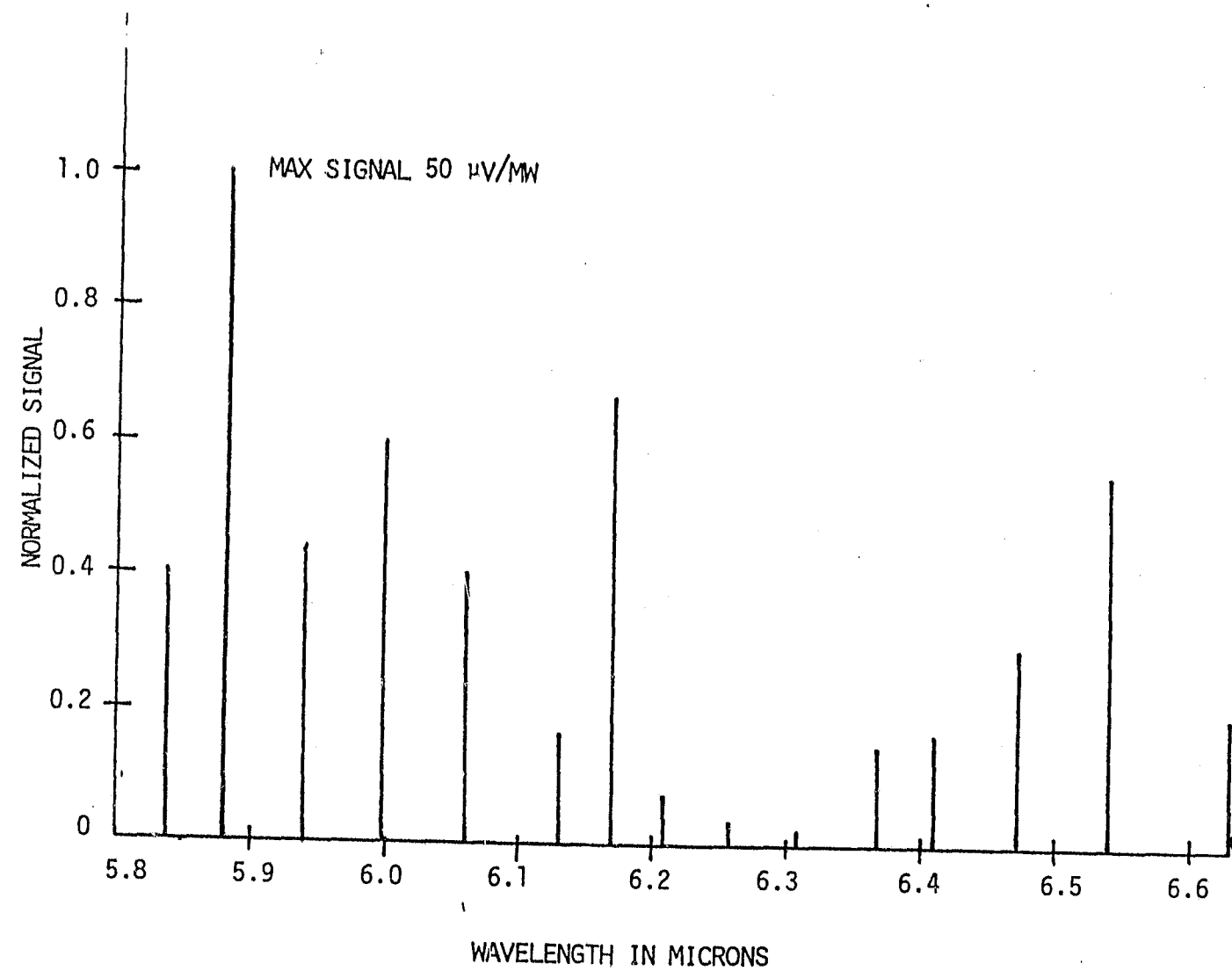


FIGURE 28. OPTOACOUSTIC SPECTRUM OF WATER VAPOR AT 6 MICRONS

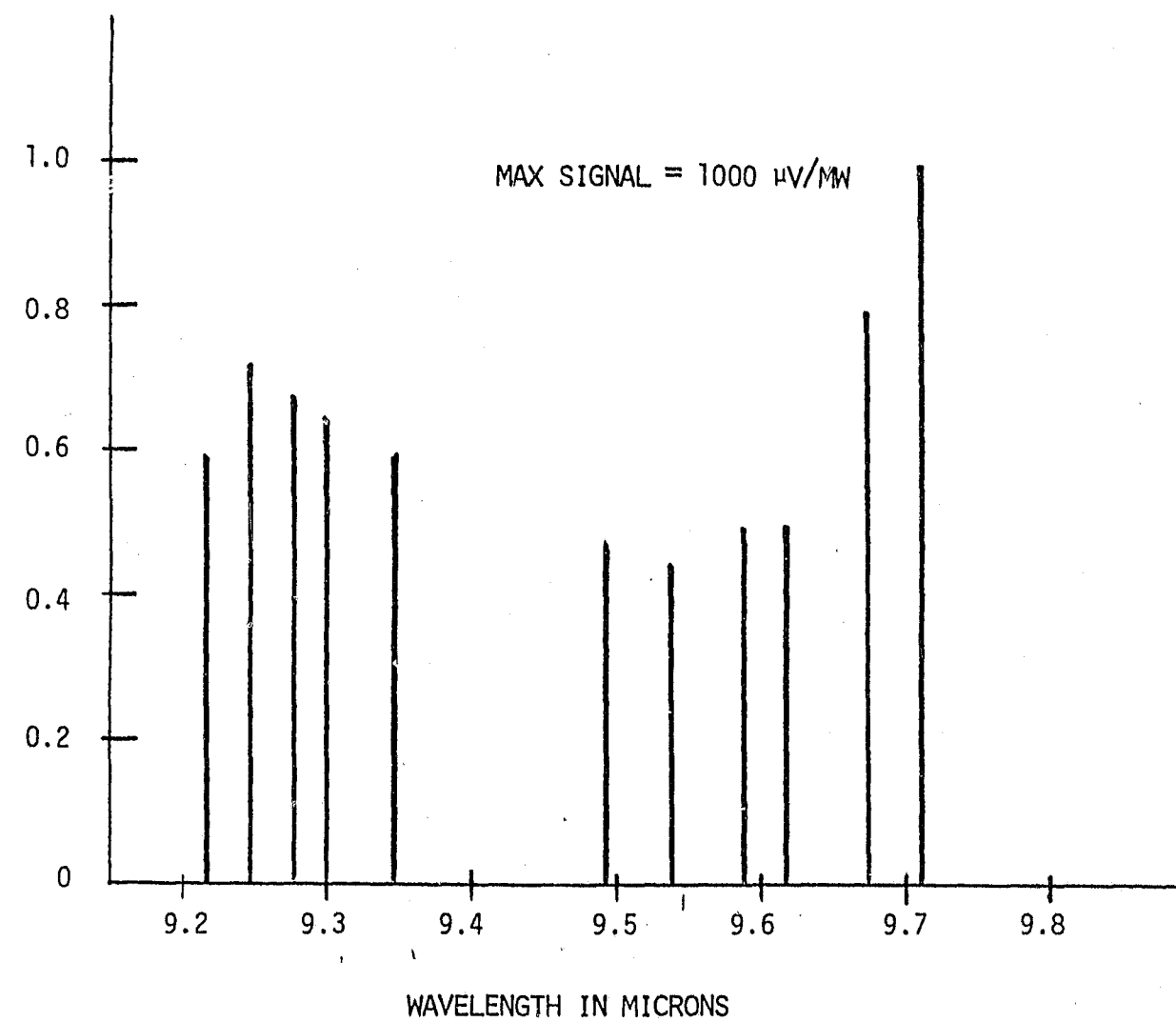


FIGURE 29. OPTOACOUSTIC SPECTRUM OF BUTANE AT 9 MICRONS

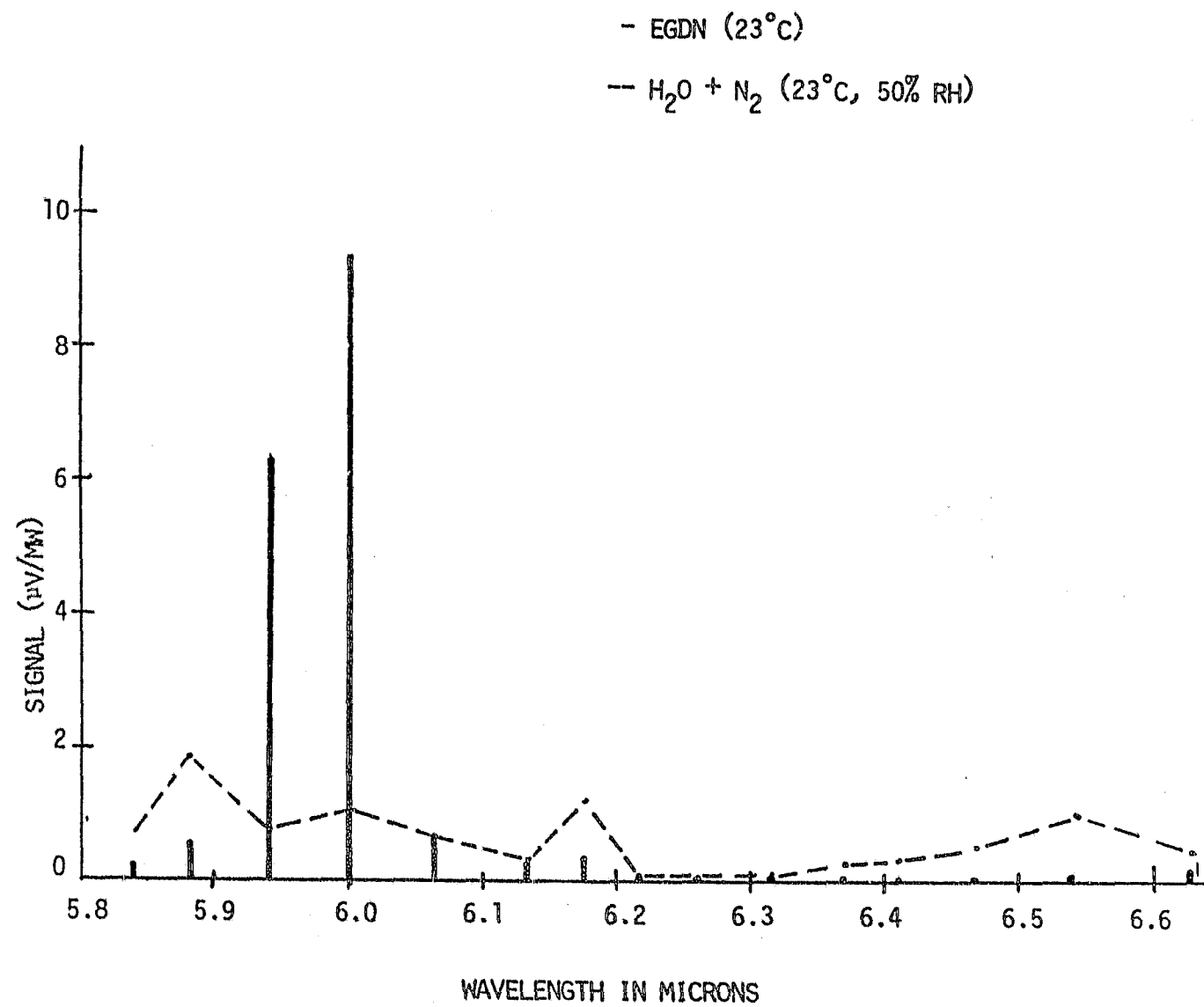


FIGURE 30. COMPARISON OF EGDN AND WATER VAPOR OPTOACOUSTIC SPECTRA
 AT 6 MICRONS (50% RELATIVE HUMIDITY)

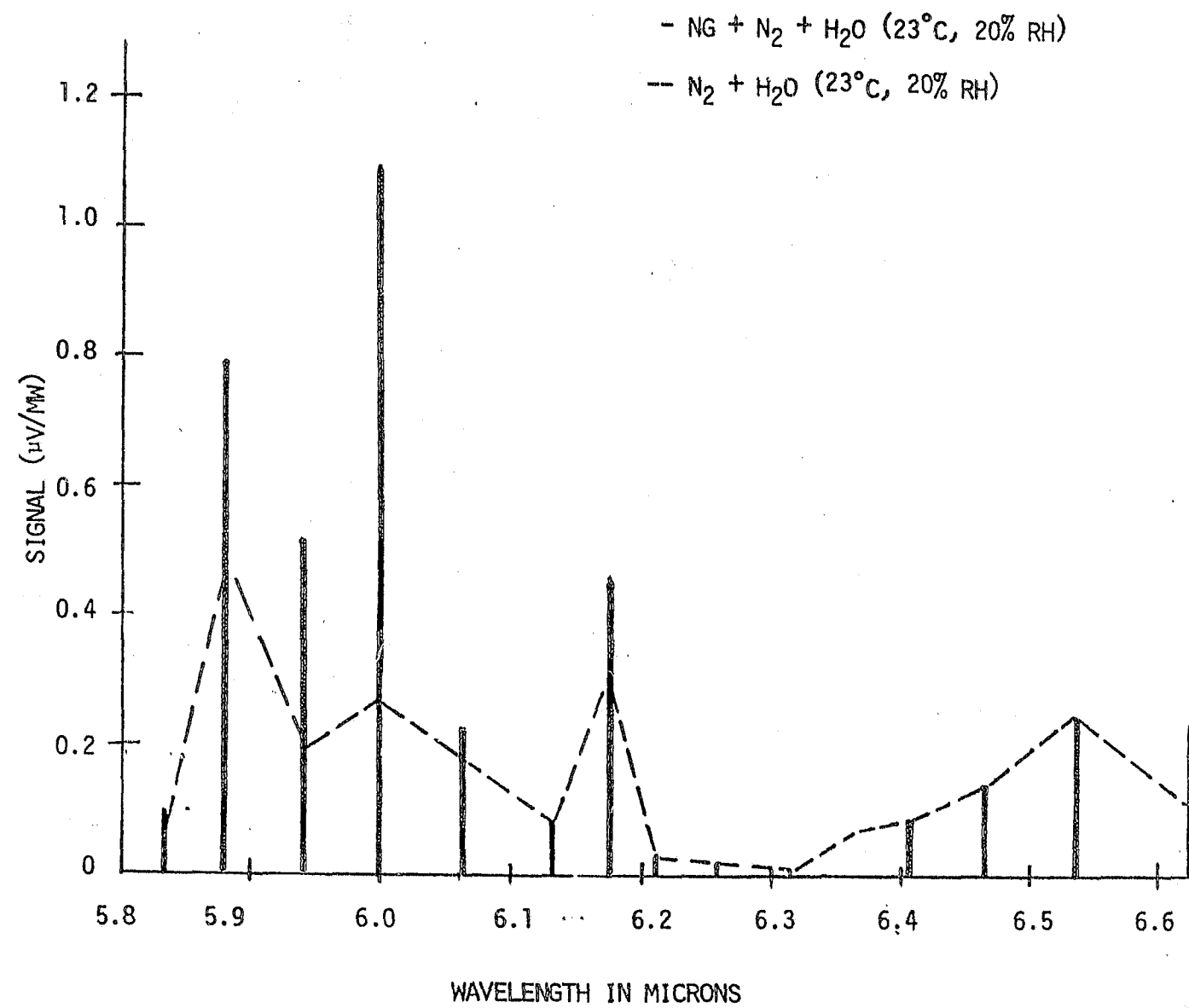


FIGURE 31. COMPARISON OF NG AND WATER VAPOR OPTOACOUSTIC SPECTRA
 AT 6 MICRONS (20% RELATIVE HUMIDITY)

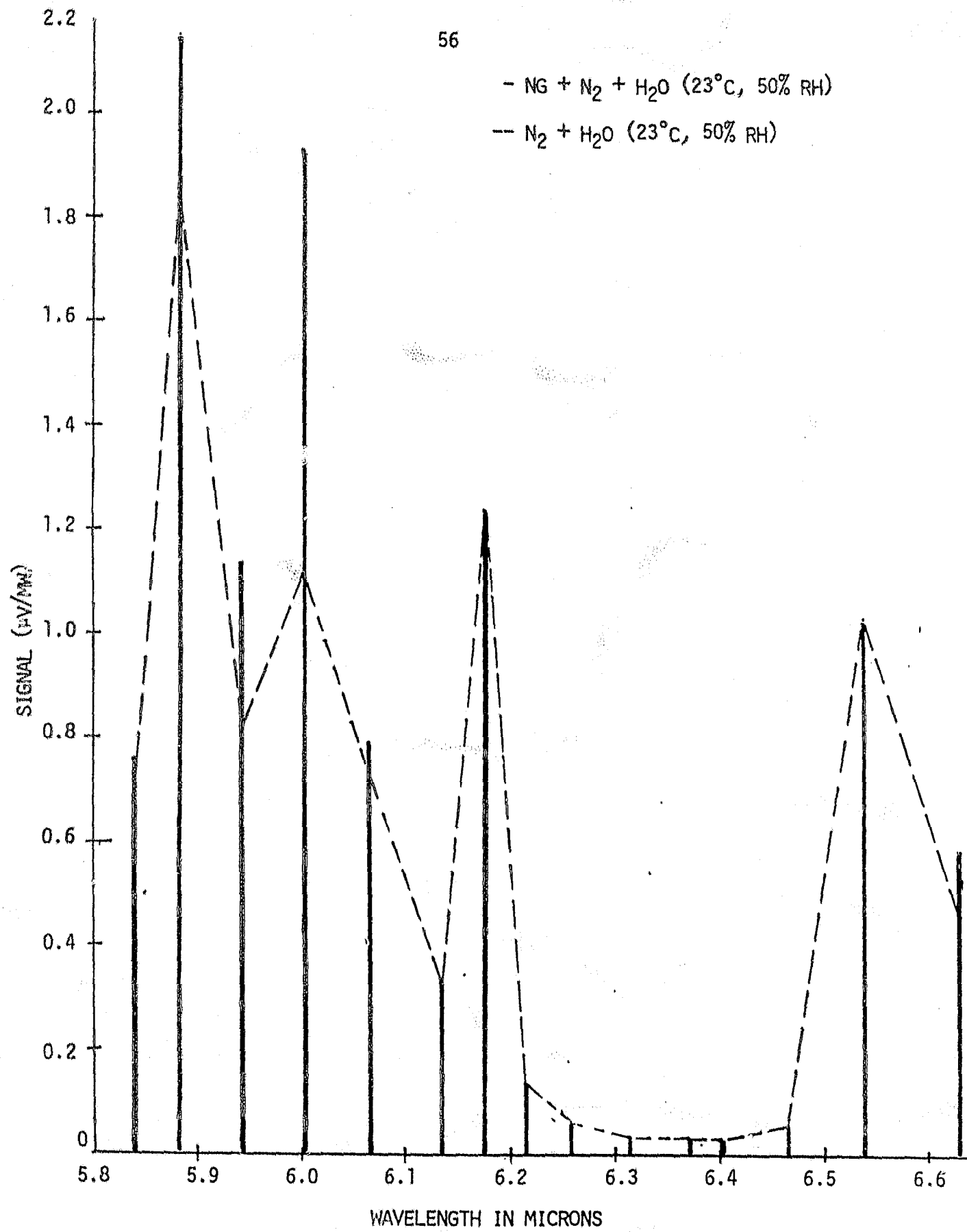


FIGURE 32. COMPARISON OF NG AND WATER VAPOR OPTOACOUSTIC SPECTRA AT 6 MICRONS (50% RELATIVE HUMIDITY)

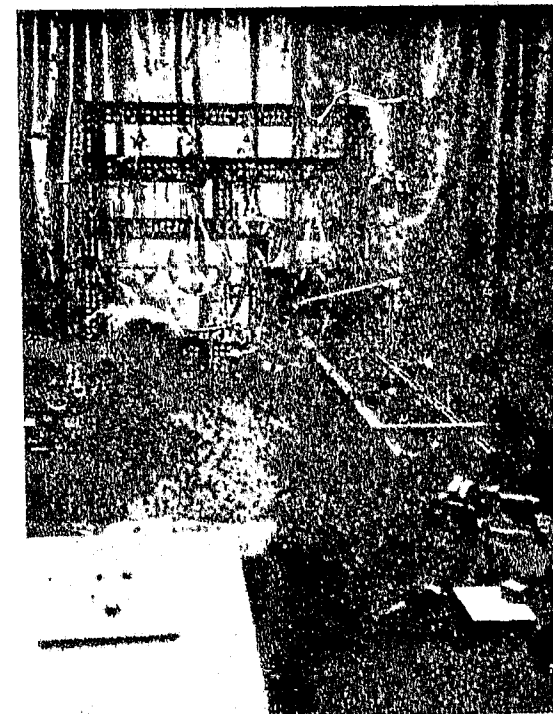


FIGURE 33a. Optoacoustic Equipment Used In The Laboratory

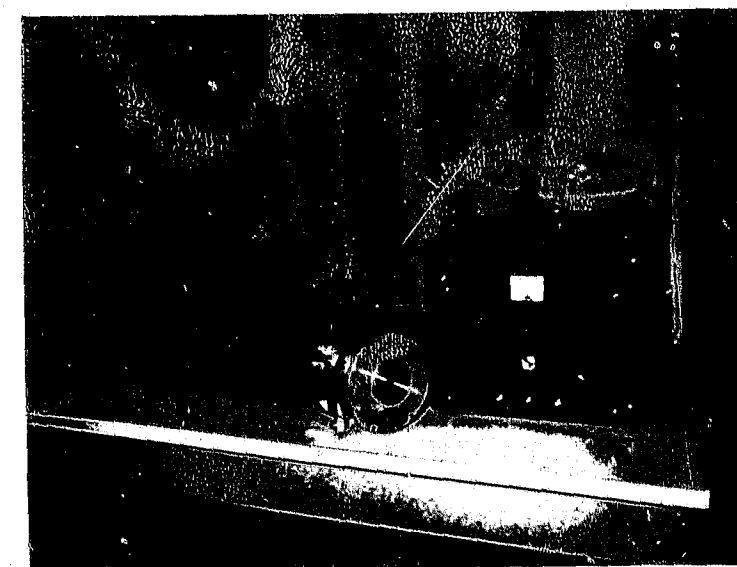


FIGURE 33b. Optoacoustic Equipment Used in Field Trial.

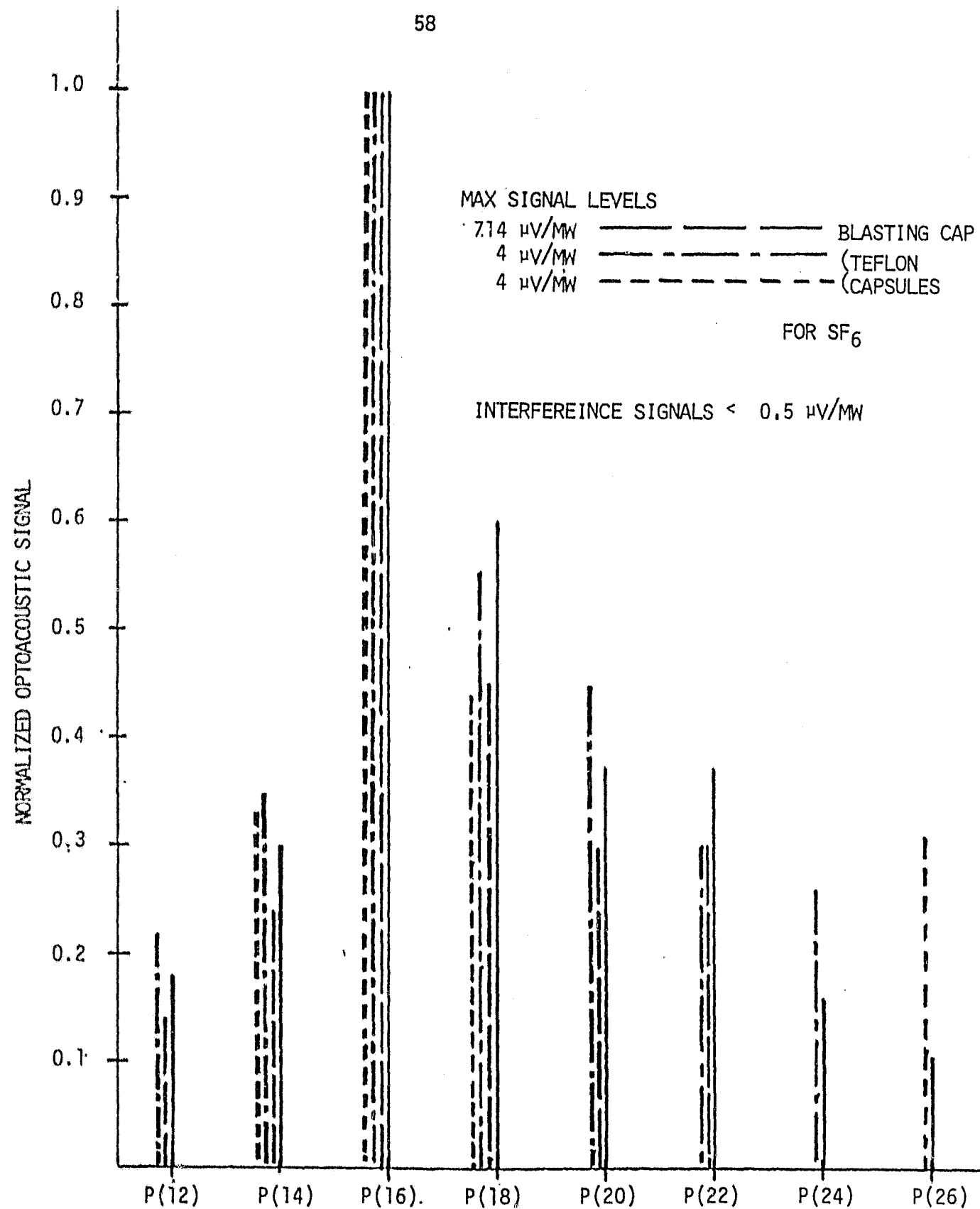


FIGURE 34. OPTOACOUSTIC DETECTION OF SF_6 IN THE 10 MICRON WAVELENGTH REGION

LIST OF TABLES

Table	Title
I	Laser Wavelengths Used in Optoacoustic Investigation
II	Analysis of Reproducibility of Data - NG and Air, 50 mw Power
III	Explosive Optoacoustic Spectra ($\mu\text{V}/\text{mw}$) in the 6 Micron Region
IV	Explosive Optoacoustic Spectra ($\mu\text{V}/\text{mw}$) in the 9 Micron Region
V	Explosive Optoacoustic Spectra ($\mu\text{V}/\text{mw}$) in the 11 Micron Region
VI	Concentration of Interfering Species (partial pressure) in Nitrogen
VII	Pollutant Optoacoustic Spectra ($\mu\text{V}/\text{mw}$) in the 6 Micron Region
VIII	Optoacoustic Efficiency of Explosives and Interfering Species at 6 Microns

TABLE I

Laser Wavelengths Used in Optoacoustic Investigation

$^{12}\text{C}^{16}\text{O}$	$^{12}\text{C}^{16}\text{O}_2$	$^{13}\text{C}^{16}\text{O}_2$
5.837 microns	9.217 microns	10.753 microns
5.880	9.247	10.800
5.941	9.303	10.833
6.002	9.352	10.850
6.063	9.455	11.065
6.132	9.501	11.107
6.174	9.550	11.149
6.213	9.601	11.194
6.258	9.655	
6.312	9.711	
6.367		
6.408		
6.465		
6.538		
6.626		

TABLE II

Analysis of Reproducibility of Data - NG and air, 50 mw Power

Line	λ	S_1	S_2	S_3	S_4	\bar{S}	$(\overline{(S-\bar{S})^2})^{1/2}$	$\frac{(\overline{(\Delta S)^2})^{1/2}}{\bar{S}} \times 100 = \delta$
P24	11.193	2.2	2.1	2.30	2.30	2.23	.083	3.7%
P22	11.171	2.2	2.3	2.20	2.10	2.20	.070	3.2
P20	11.149	2.4	2.3	2.20	2.20	2.28	.083	3.6
P18	11.127	2.4	2.38	2.30	2.20	2.32	.078	3.3
P16	11.106	2.1	2.20	2.10	2.10	2.13	.043	2.0
P14	11.085	2.3	2.30	2.20	2.20	2.25	.050	2.2
R14	10.816	.64	.60	.60	.60	.61	.021	3.5
R16	10.800	.50	.52	.44	.44	.475	.046	9.6
R18	10.783	.46	.36	.44	.44	.425	.038	5.9
R20	10.768	.46	.46	.44	.44	.45	.010	2.2
R22	10.752	.36	.36	.38	.36	.365	.008	2.3

$$(\delta^2)^{1/2} = 4.8\%$$

Analysis of Reproducibility of Data

NG + Air

50 mw Power

TABLE III

Explosive Optoacoustic Spectra ($\mu\text{V}/\text{mw}$) in the 6 Micron Region

<u>WAVELENGTH</u>	<u>NG</u>	<u>EGDN +10%NG</u>	<u>DNT</u>	<u>TNT</u>	<u>TOVEX</u>	<u>RDX</u>	<u>PETN</u>	<u>DYNAMITE</u>
6.626 μ	0.8	0.8	1.6	0.2	4.8	3.2	2.4	4.8
6.538	0	0	3.0	3.2	12.2	5.2	6.2	6.0
6.465	0	0	1.6	2.1	5.4	3.1	2.8	3.6
6.408	0	0	1.1	0.8	2.8	1.3	1.1	1.5
6.367	0	0	0.8	0.8	2.3	1.3	1.5	2.2
6.312	0	0	0	0	0.3	0.3	0	0
6.258	0	0	0	0	0.5	0.3	0	0
6.213	0	0	0.4	0.5	1.1	1.0	0.2	0.5
6.174	1.0	2.2	2.0	5.8	13.3	5.8	6.0	3.5
6.132	0	1.4	0.3	0.6	2.6	1.1	1.3	2.0
6.063	0.3	3.9	1.3	2.8	6.2	3.6	1.1	3.6
6.002	5.3	60.5	4.6	2.6	10.9	5.3	4.3	7.6
5.941	2.1	41.2	3.2	3.0	8.5	3.5	2.7	6.0
5.880	2.0	3.3	2.9	7.2	16.7	7.2	7.4	7.2
5.837	0.1	1.2	1.1	1.6	6.1	3.1	2.3	3.0

TABLE IV

Explosive Optoacoustic Spectra ($\mu\text{V}/\text{mw}$) in the 9 Micron Region

<u>Wavelength</u>	<u>NG</u>	<u>EGDN</u>	<u>DNT</u>
9.711 μ	1.7	2.5	0.8
9.655	1.7	2.2	0.6
9.601	2.2	3.2	0.8
9.550	2.2	5.0	1.0
9.501	2.2	5.0	1.1
9.455	-	4.0	1.0
9.352	0.75	2.0	.55
9.303	0.5	1.5	.35
9.247	0.25	1.0	.30
9.217	-	0.5	.20

TABLE V

Explosive Optoacoustic Spectra ($\mu\text{v}/\text{mw}$) in the 11 Micron Region

<u>Wavelength</u>	<u>NG(45°C)</u>	<u>NG(23°C)</u>	<u>EGDN(45°C)</u>	<u>EGDN(23°C)</u>
11.194 μ	6.5	0.4	6.2	0.6
11.149	5.2	0.4	7.0	0.6
11.107	4.6	0.4	6.5	0.55
11.065	3.3	0.35	5.3	0.5
10.850	-	0.12	-	0.23
10.833	1.5	-	1.5	-
10.800	1.3	0.12	0.8	0.23
10.753	1.0	0.12	0.5	0.23

TABLE VI

Concentration of Interfering Species (partial pressure) in Nitrogen

<u>Interfering Species</u>	<u>Concentration</u>
NO	16 ppm
NO ₂	6.1
CH ₄	10
C ₄ H ₁₀	8.8
Water Vapor	~ 57,000

TABLE VII

Pollutant Optoacoustic Spectra ($\mu\text{V}/\text{mw}$) in the 6 Micron Region

Wavelength (Microns)	Butane	Methane	Nitric Oxide	Nitrogen Dioxide	Water
6.626	2.50	0.17	2.38	9.17	12.5
6.538	1.67	0.67	2.37	0	28.0
6.465	2.50	1.59	0.39	5.50	15.0
6.408	2.40	0.75	1.08	3.08	8.5
6.367	0.72	0.90	0.28	2.00	7.5
6.312	0.13	0.47	0.25	1.16	1.0
6.258	0.20	0.09	0.67	0.94	1.5
6.213	0.25	0.29	0.65	2.01	3.5
6.174	1.75	1.08	1.87	8.37	33.5
6.132	0.30	0.21	0.25	1.75	9.0
6.063	0.28	0.42	0.34	3.43	20.0
6.002	1.43	0	0	4.17	30.0
5.941	0.91	0.19	0.22	3.18	22.0
5.880	1.16	0.91	0.14	8.64	50.0
6.837	0.75	2.10	0	9.44	20.0

TABLE VIII

Optoacoustic Efficiency of Explosives and
Interfering Species at 6 Microns

Molecule	Max. Normalized Optoacoustic Signal ($\mu\text{V}/\text{mw}$)	Molecular Concentration (ppm)	Max. normalized Optoacoustic Signal per ppm ($\mu\text{V}/\text{mw}/\text{ppm}$)
NG	5.3	0.62	8.55
EGDN	60.5	53	1.14
DNT	4.6	92	0.05
NO	2.38	16	0.15
NO ₂	9.44	6.1	1.55
H ₂ O	50	47 x 10 ³ (39°C, 50% RH)	0.001
CH ₄	2.1	10	0.21
Butane	2.5	8.8	0.28

Results calculated using the following data:

Explosive	Number density at 45°C for vapor in equilibrium with explosive
NG	1.43 x 10 ¹³ cm ⁻³
EGDN	1.22 x 10 ¹⁵
DNT	2.13 x 10 ¹⁵

1 ppm in air at 1 atm, 45°C corresponds to 2.3 x 10¹³ cm⁻³

APPENDIX I

A Rate Equation Description Of A
Two Level Optoacoustic System

In the interest of completeness, we provide here a rate equation description of a simple two level model of an optoacoustic system. In this model, the molecular system interacts resonantly with incident radiation and transitions between the two levels are stimulated. In addition, de-excitation from the upper level occurs because of fluorescence (spontaneous emission, with rate τ_R^{-1}) and also because of collisions (with rate τ_C^{-1}). The optoacoustic signal is proportional to $N_2\tau_C^{-1}$ where N_2 is the number of molecules in the upper state, per unit volume. The power levels required for excitation, the behavior of the system when near saturation and the desirability of using the second harmonic signal are topics also mentioned briefly in passing.

Let us consider a two level system, and

$$\text{Let } N = \text{number of molecules/cm}^3 = N_1 + N_2$$

$$\text{where } N_1 = \text{number of molecules/cm}^3 \text{ in the lower state}$$

$$\text{and } N_2 = \text{number of molecules/cm}^3 \text{ in the upper state}$$

The rate equation description of the system may be written as

$$\frac{dN_1}{dt} = -B_{12} \frac{I_\nu h\nu}{c} N_1 + B_{21} \frac{I_\nu h\nu}{c} N_2 + \left(\frac{1}{\tau_R} + \frac{1}{\tau_C} \right) N_2 \quad (1)$$

$$\frac{dN_2}{dt} = -B_{21} \frac{I_\nu h\nu}{c} N_2 + B_{12} \frac{I_\nu h\nu}{c} N_1 - \left(\frac{1}{\tau_R} + \frac{1}{\tau_C} \right) N_2 \quad (2)$$

where $B_{12} = B_{21}$ = Einstein's Coefficient For Stimulated Emission and Absorption

ν = frequency of radiation interacting resonantly with the molecular system

I_ν = number of photons/cm²/sec of energy $h\nu$

τ_R = radiation lifetime of upper state

τ_C = collisional lifetime of upper state

For convenience these equations can be combined and slightly rewritten as

$$\frac{d}{dt} (N_2 - N_1) = -B(N_2 - N_1)I_\nu - 2\tau^{-1} N_2 \quad (3)$$

where

$$B = B_{12} \frac{h\nu}{c}$$

$$\tau^{-1} = \left(\frac{1}{\tau_R} + \frac{1}{\tau_C} \right)$$

We note in passing that

$$B_{12} = \frac{\pi^2 c^3}{\Delta\nu h\nu^3} A_{21} = \frac{\pi^2 c^3}{\Delta\nu h\nu^3 \tau_R}$$

We may safely assume that steady-state conditions are always attained, i.e., for any I_ν , the system has ample time to adjust itself to steady-state conditions appropriate to that value. This means that we can take

$$\frac{d}{dt} (N_2 - N_1) = 0 \quad \text{and equation (3) yields}$$

$$N_2 = \frac{BN I_\nu}{2BI_\nu + 2\tau^{-1}} \quad (4)$$

The acoustic signal is proportional to $N_2\tau_C^{-1}$ and we have accordingly

$$\text{that the acoustic signal} \propto N_2\tau_C^{-1} = \frac{BN I_\nu \tau_C^{-1}}{2BI_\nu + 2\tau^{-1}} \quad (5)$$

In the case where the incident radiation is modulated at frequency ω so that

$$I_\nu = I_0(1 + \delta \sin\omega t) \quad \text{where } 0 \leq \delta \leq 1 \quad (6)$$

we can consistently write

$$N_2 \tau_C^{-1} = \frac{BN I_0 (1 + \delta \sin\omega t) \tau_C^{-1}}{2BI_0 (1 + \delta \sin\omega t) + 2\tau^{-1}} \quad (7)$$

Expanding in powers of $\delta \sin\omega t$ and retaining only terms up to the second power of $(\delta \sin\omega t)$, we have

$$N_2 \tau_c^{-1} = \frac{B N I_0 \tau_c^{-1}}{2 B I_0 + 2 \tau_c^{-1}} - \frac{4 B^2 I_0^2 N \tau_c^{-1} \delta^2}{[2 B I_0 + 2 \tau_c^{-1}]^3} + \frac{2 \tau_c^{-2} B N I_0}{(2 B I_0 + 2 \tau_c^{-1})^2} \delta \sin \omega t + \frac{4 B^2 I_0^2 N \tau_c^{-1}}{(2 B I_0 + 2 \tau_c^{-1})^3} \delta^2 \sin 2 \omega t + \dots \quad (8)$$

Insofar as the $\sin \omega t$ term is concerned, we see that for very small I_0 , $B I_0 \ll \tau_c^{-1}$ and

$$\frac{2 \tau_c^{-2} B N I_0}{(2 B I_0 + 2 \tau_c^{-1})^2} \delta \rightarrow \frac{1}{2} \left(\frac{\tau_c}{\tau_c} \right)^2 B N I_0 \delta \quad (9)$$

But when I_0 becomes very large, then

$$\frac{2 \tau_c^{-2} B N I_0}{(2 B I_0 + 2 \tau_c^{-1})^2} \delta \rightarrow \frac{1}{2} \tau_c^{-2} \frac{N}{B I_0} \delta \quad (10)$$

It is quite transparent that $B I_0$ should be large but not larger than τ_c^{-1} . This can be demonstrated also by solving (10) for the optimum value of $B I_0$. Actually $B I_0 = \frac{1}{\tau_c}$ or the reciprocal of the lifetime as specified by interaction with radiation and the optimum condition merely says (qualitatively) that we should not pump harder than we can deplete the upper state by collisional process.

Depending on the partial pressure of the absorbing gas, the presence or absence of other gases, and the influence of wall collisions, τ might be of the order of, say, 10^{-6} sec. and it found that saturation sets in at quite low powers of the order of fractions of a watt/cm². This is in agreement with our experience in our high resolution saturation spectra of SF₆ and of I₂¹²⁹.

Furthermore the manner in which saturation occurs is of interest. In equation (8), the dominant D.C. term has I_0 to the same power in the numerator and in the denominator. Unnecessarily high values of I_0 might not bring correspondingly higher signal values but there are no penalties either. This is different for the other terms. In particular, the a.c. term at frequency ω saturates according to I_0^{-1} and so does the second harmonic term. It is important therefore in practice to avoid using unnecessarily high incident powers.

Scattering and absorption at the window would result in a spurious signal also at a frequency of ω and it has been suggested that detection of the second harmonic might provide the means for discriminating against that spurious signal. However, from equation (8) we note that as saturation sets in the two terms have the following behavior.

$$\frac{2 \tau_c^{-2} B N I_0}{(2 B I_0 + 2 \tau_c^{-1})^2} \delta \sin \omega t \rightarrow \frac{1}{2} \frac{\tau_c^{-2} \delta}{B I_0} \sin \omega t \quad (12)$$

$$\frac{4 B^2 I_0^2 N \tau_c^{-1}}{(2 B I_0 + 2 \tau_c^{-1})^3} \delta^2 \sin 2 \omega t \rightarrow \frac{1}{2} \frac{\tau_c^{-1} \delta^2}{B I_0} \sin 2 \omega t \quad (13)$$

The amplitude of the second harmonic term is smaller by a factor of τ_c^{-1} which can be as large as 10^7 !

APPENDIX II

COLLECTION OF LOW RESOLUTION INFRARED ABSORPTION
SPECTRA FOR EXPLOSIVES AND INTERFERING SPECIES

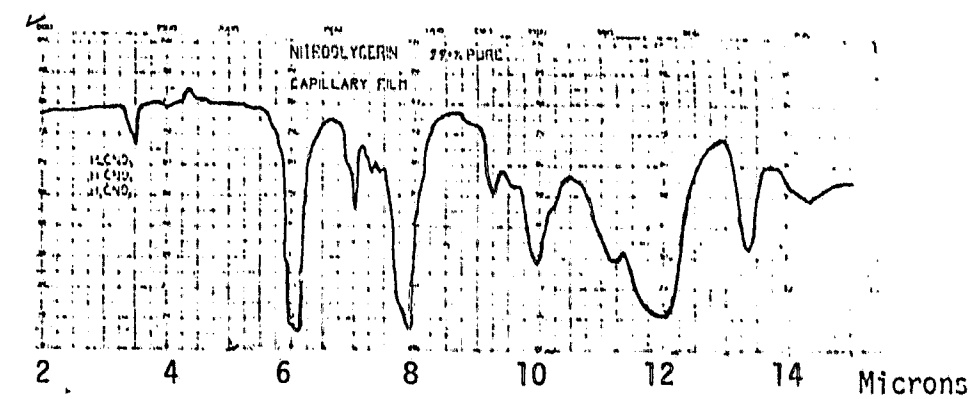


Figure A1. Low Resolution Absorption Spectrum of NG (Ref. 3)

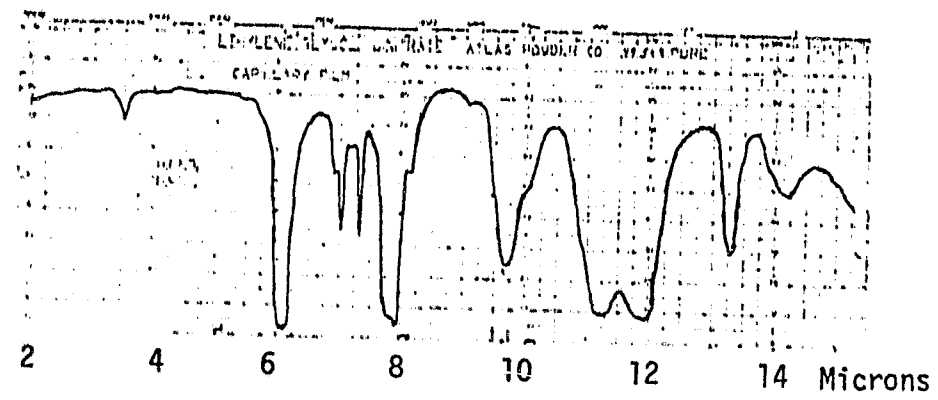


Figure A2. Low Resolution Absorption Spectrum of EGDN (Ref. 3)

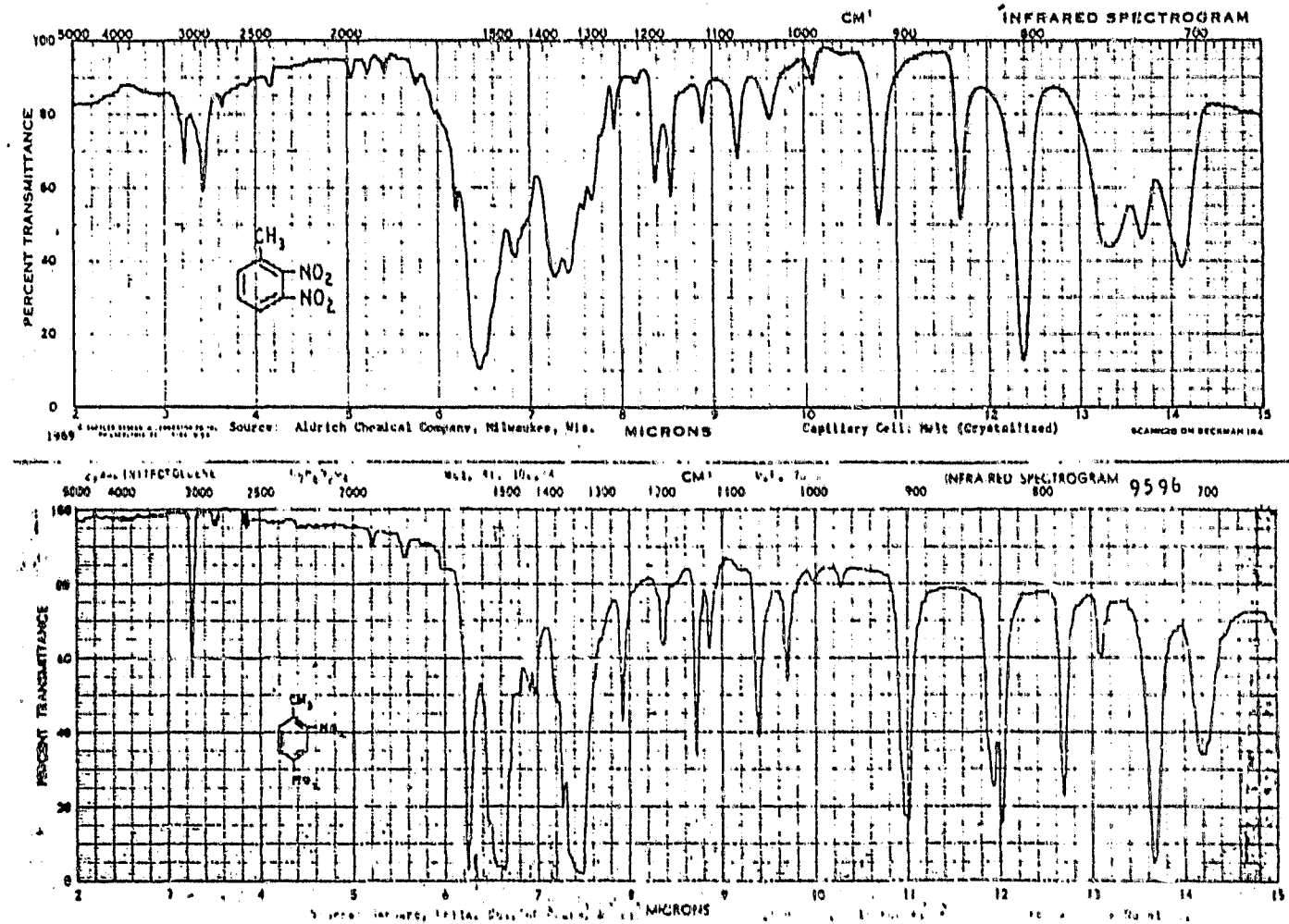


Figure A3. Low Resolution Absorption Spectra of 2,3 DNT, 2,4 DNT, 2,6 DNT, and 3,4 DNT (Ref. 4)

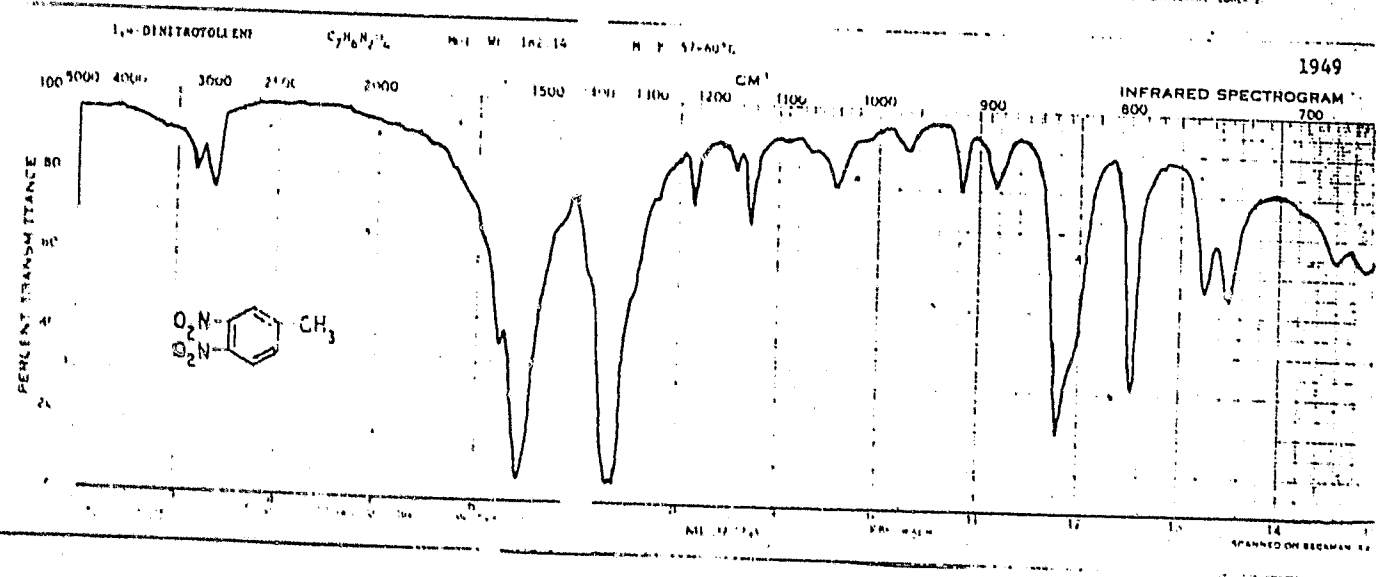
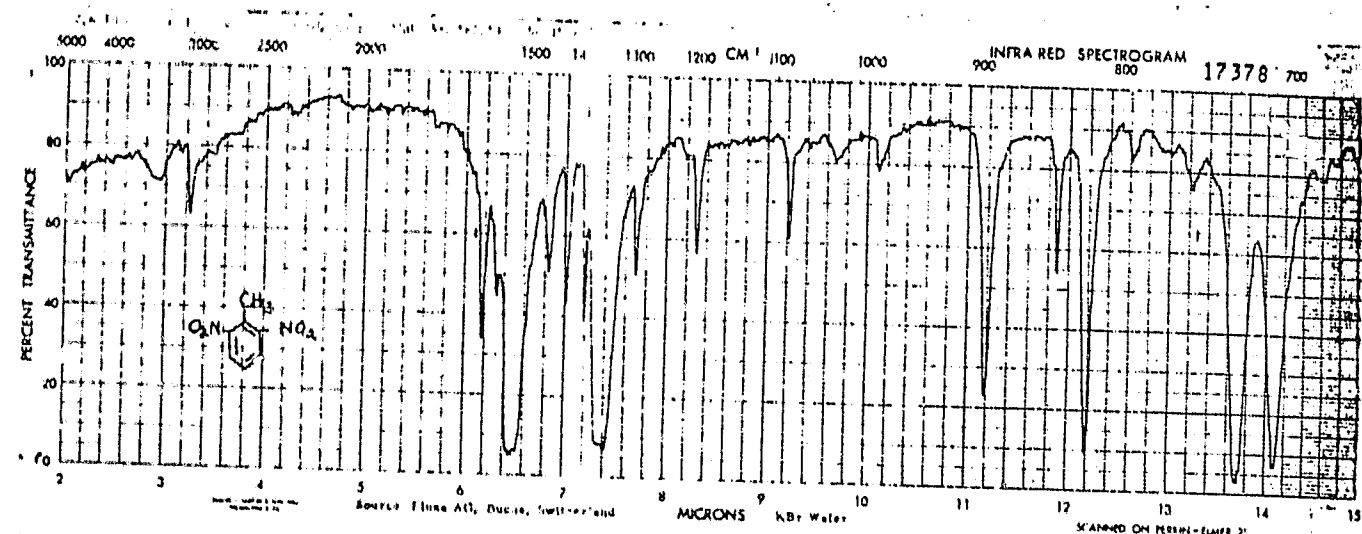


Figure A3. Low Resolution Absorption Spectra of 2,3 DNT, 2,4 DNT, 2,6 DNT, and 3,4 DNT (Ref. 4) (Cont'd.)

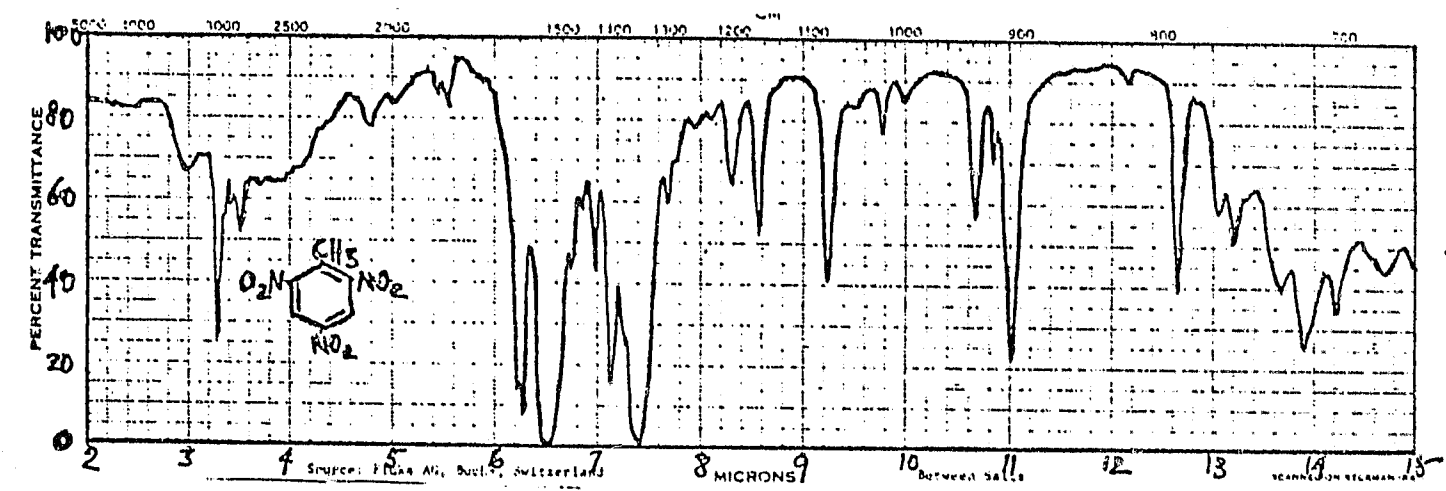


Figure A4. Low Resolution Absorption Spectrum of TNT (Ref. 4)

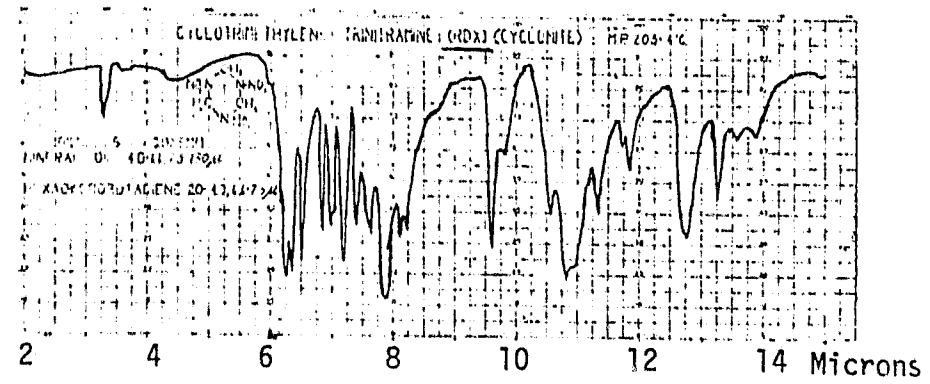


Figure A5. Low Resolution Absorption Spectrum of RDX (Ref. 3)

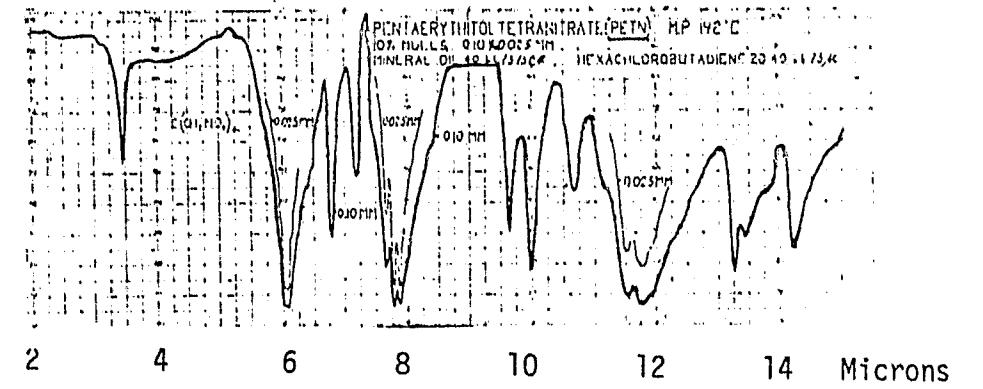


Figure A6. Low Resolution Absorption Spectrum of PETN (Ref. 3)

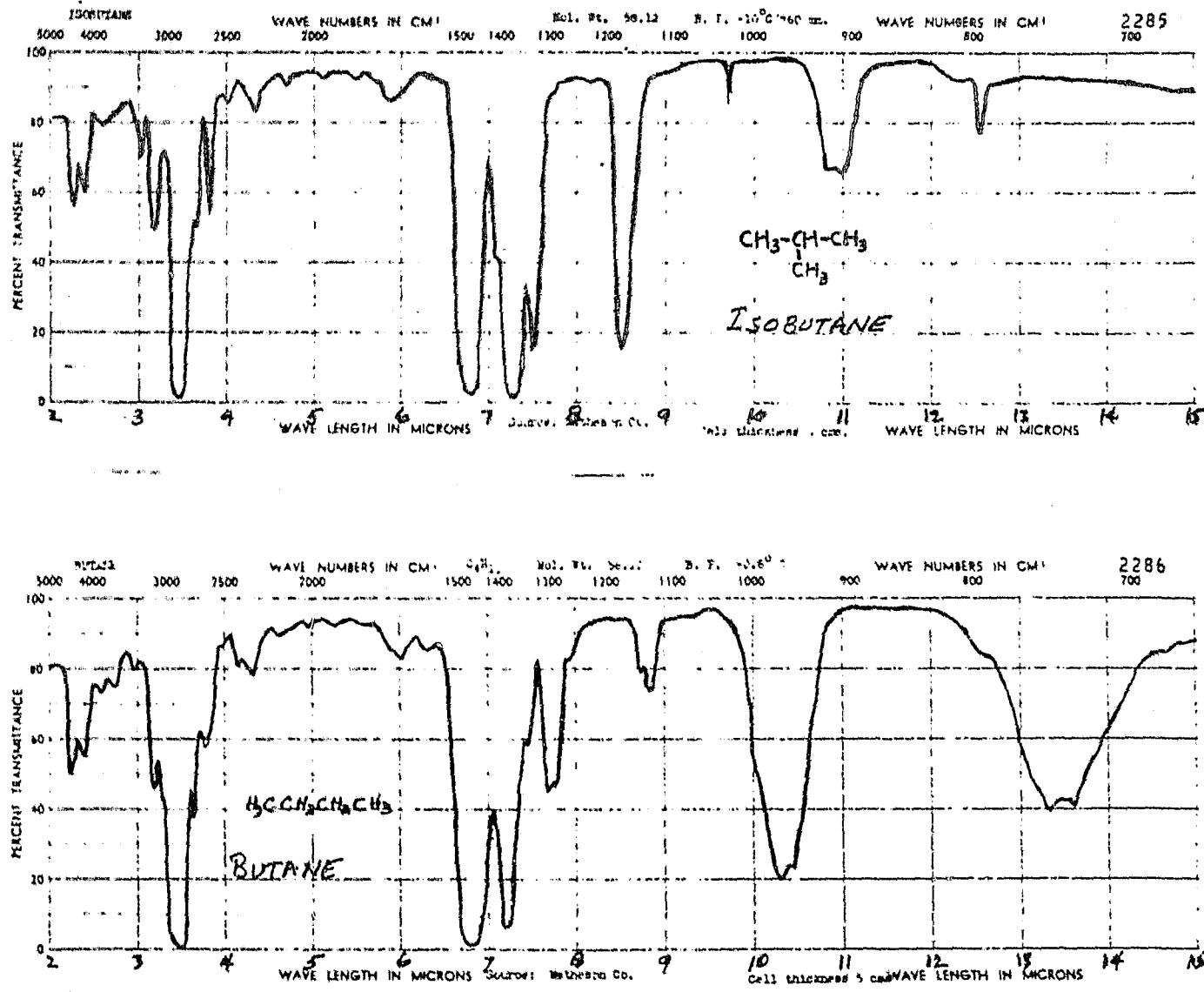


Figure A7. Low Resolution Absorption Spectrum of n-Butane and Iso-butane (Ref. 4)

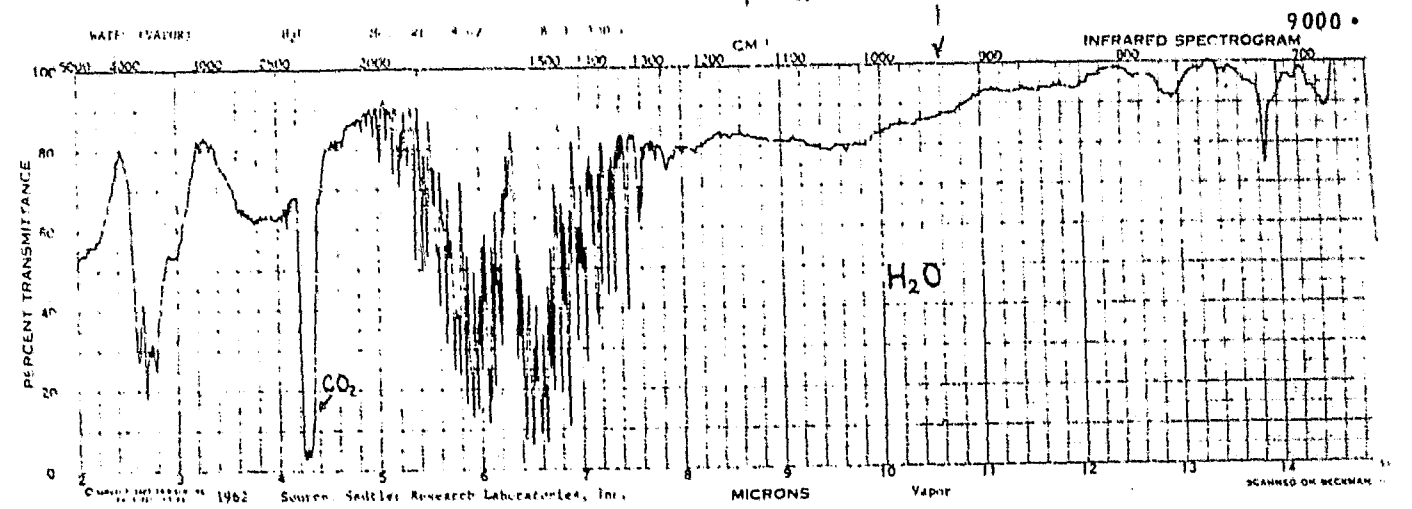


Figure A8. Low Resolution Absorption Spectrum of Water Vapor (Ref. 4)

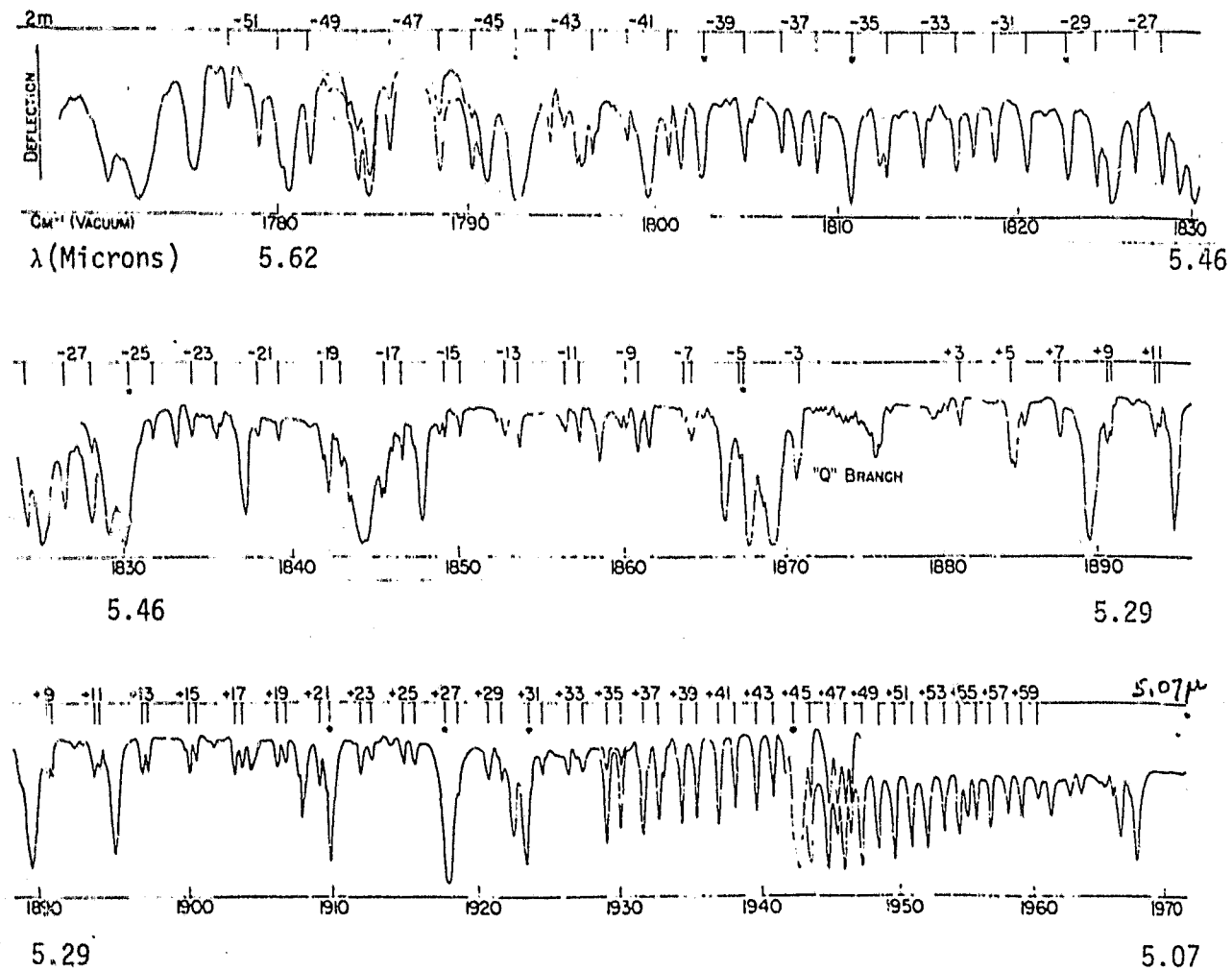
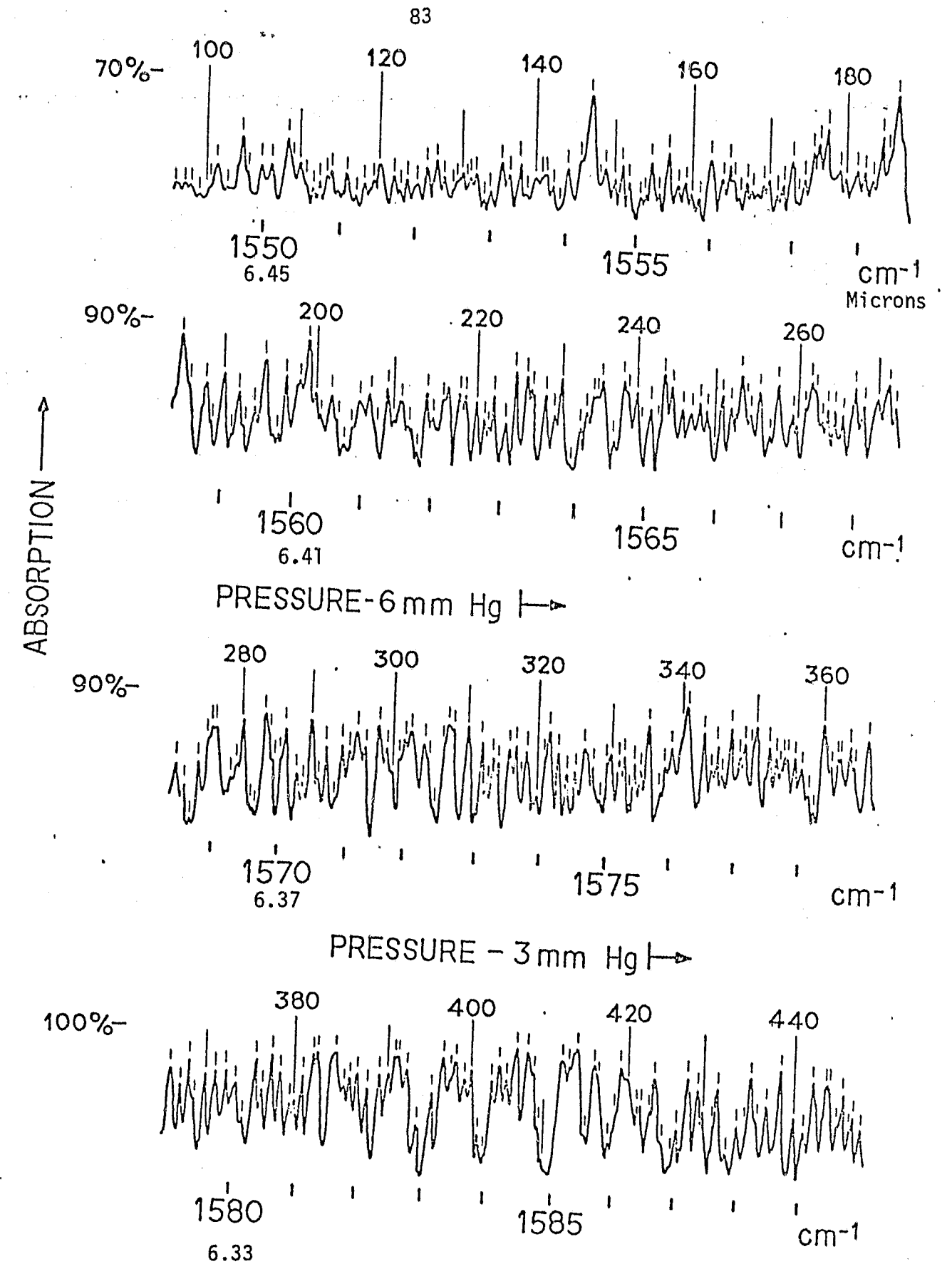


Figure A9. High Resolution Absorption Spectrum of NO (Ref. 5)

Figure A10. High Resolution Absorption Spectrum of NO₂ (Ref. 6)

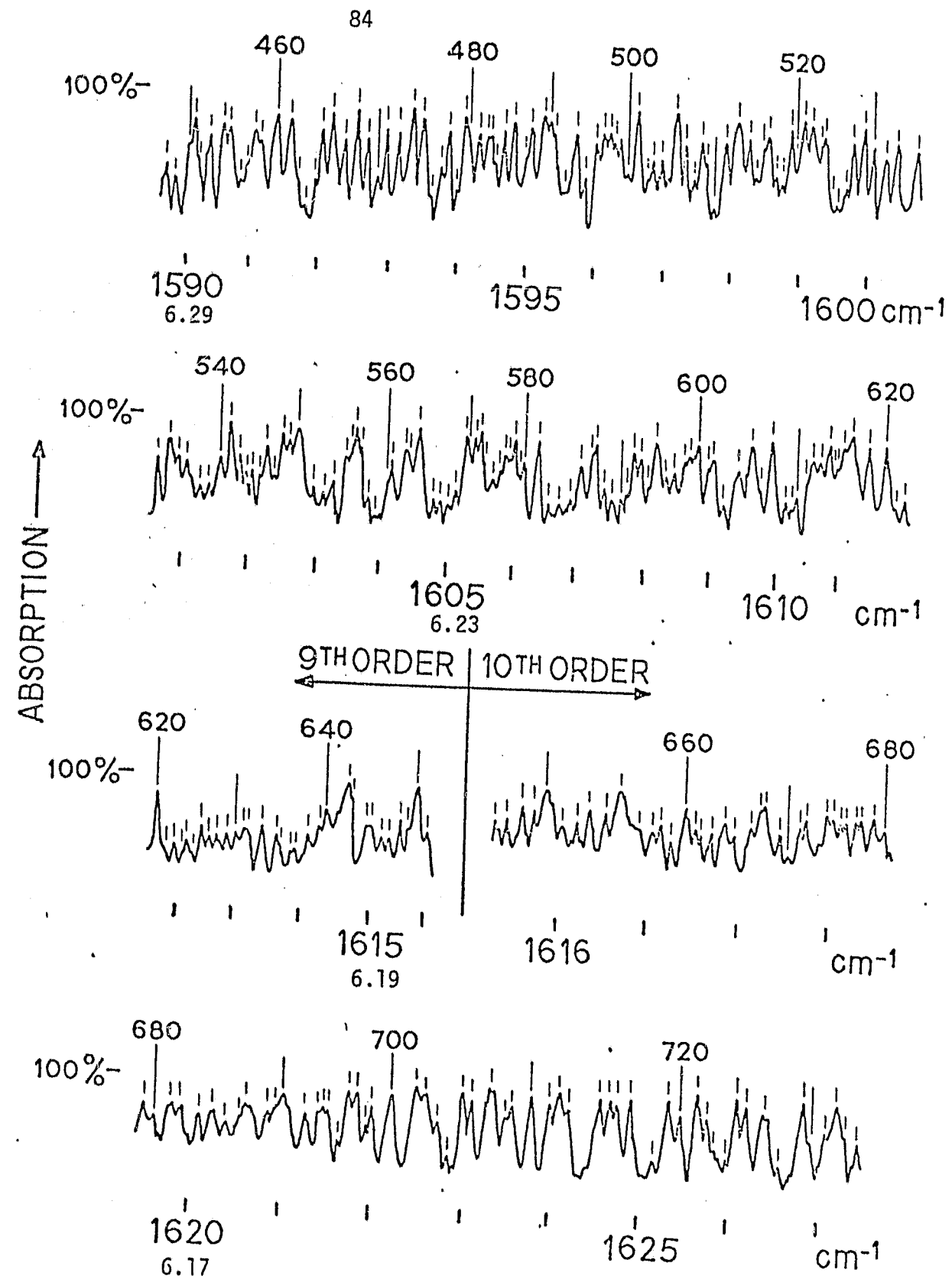


Figure A10. High Resolution Absorption Spectrum of NO_2 (Ref. 6) (Cont'd)

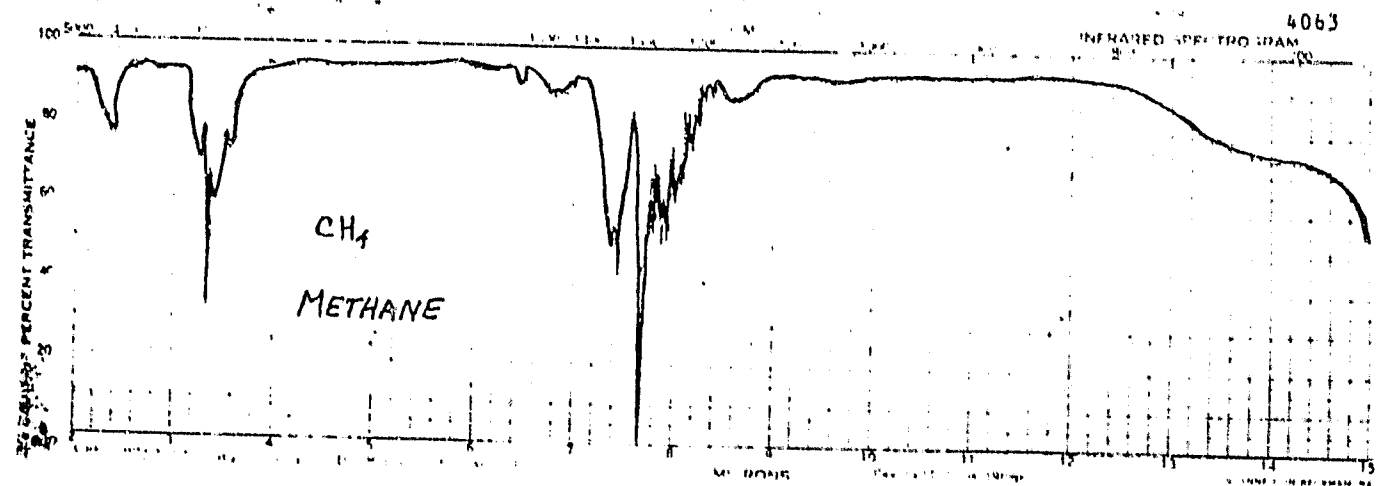


Figure A11. Low Resolution Absorption Spectrum of Methane (Ref. 4)

References

1. Urbanski, Tadeusz, Chemistry and Technology of Explosives, Pergamon Press, (1964).
2. Coates, A. D., Eli Freeman, Lester P. Kuhn, Characteristics of Certain Military Explosives, Ballistics Research Laboratory, Aberdeen Proving Ground, Md. BRL Report No. 1507, November 1970.
3. Pristera, F., M. Halik, A. Castelli, and W. Fredericks, "Analysis of Explosives Using Infrared Spectroscopy", *Anal. Chem.* Vol. 32, pp. 495-508, (April 1960).
4. Standard IR Spectra, Sadtler Research Laboratories, Inc., Philadelphia, Pa.
5. Shaw, J. H., "Nitric Oxide Fundamental", *J. Chem. Phys.*, Vol. 24, pp. 399-402 (Feb. 1956).
6. Hurlock, S. C., K. N. Rao, L. A. Weller, and P. K. L. Yin, "High Resolution Spectrum and Analysis of the ν_2 Band of $^{14}\text{N}^{16}\text{O}_2$ ", *J. Mol. Spectrosc.*, Vol. 48, pp. 372-394 (Nov. 1973).

END